

Accepted Manuscript

Water-stable metal-organic frameworks for aqueous removal of heavy metals and radionuclides: A review

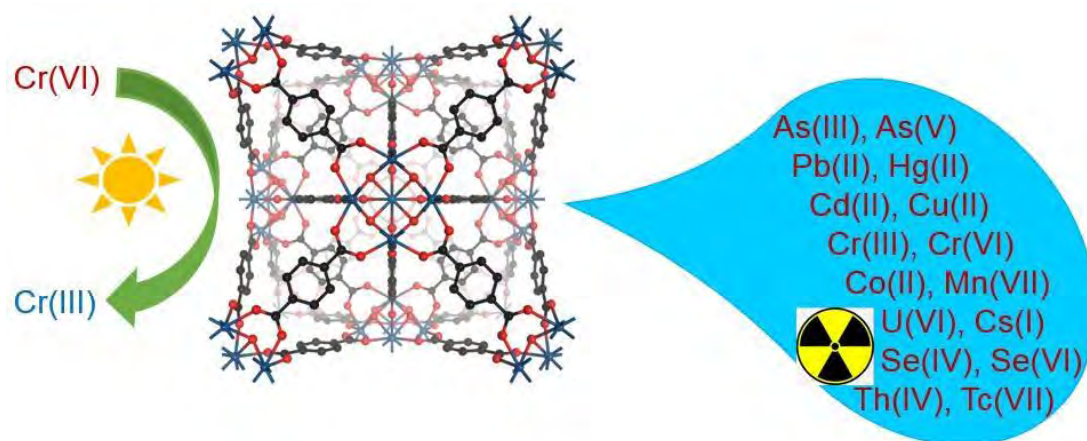


Mingbao Feng, Peng Zhang, Hong-Cai Zhou, Virender K. Sharma

PII: S0045-6535(18)31189-5
DOI: 10.1016/j.chemosphere.2018.06.114
Reference: CHEM 21646
To appear in: *Chemosphere*
Received Date: 22 March 2018
Accepted Date: 16 June 2018

Please cite this article as: Mingbao Feng, Peng Zhang, Hong-Cai Zhou, Virender K. Sharma, Water-stable metal-organic frameworks for aqueous removal of heavy metals and radionuclides: A review, *Chemosphere* (2018), doi: 10.1016/j.chemosphere.2018.06.114

This is a PDF file of an unedited manuscript that has been accepted for publication. As a service to our customers we are providing this early version of the manuscript. The manuscript will undergo copyediting, typesetting, and review of the resulting proof before it is published in its final form. Please note that during the production process errors may be discovered which could affect the content, and all legal disclaimers that apply to the journal pertain.



Catalysis

Adsorption

Green MOFs to capture heavy metals and radionuclides
for sustainable water purification

Water-stable metal-organic frameworks for aqueous removal of heavy metals and radionuclides: A review

Mingbao Feng,^a Peng Zhang,^b Hong-Cai Zhou,^b Virender K. Sharma^{*,a}

^a Department of Environmental and Occupational Health, School of Public Health, Texas A&M University, College Station, Texas 77843, USA

^b Department of Chemistry, Texas A&M University, College Station, Texas 77842-3012, USA

* Corresponding author: Virender K. Sharma.

Email address: vsharma@sph.tamhsc.edu

Abstract

Heavy metals and radionuclides in water are a global environmental issue, which has been receiving considerable attention worldwide. Water-stable MOFs are green and recyclable materials to eliminate the environmental impacts caused by the hazardous heavy metal ions and radionuclides in water. This paper presents a systematical review on the current status of water-stable MOFs that capture and convert a wide range of heavy metal ions (e.g., As(III)/As(V), Pb(II), Hg(II), Cd(II), and Cr(III)/Cr(VI)) and radionuclides (e.g., U(VI), Se(IV)/Se(VI) and Cs(I)) in aqueous solution. Water-stable MOFs and MOF-based composites exhibit the superior adsorption capability for these metal species in water. Significantly, MOFs show high selectivity in capturing target metal ions even in the presence of multiple water constituents. Mechanisms involved in capturing metal ions are described. MOFs also have excellent catalytic performance (photocatalysis and catalytic reduction by formic acid) for Cr(VI) conversion to Cr(III). Future research is suggested to provide insightful guidance to enhance the performance of the MOFs in capturing target pollutants in aquatic environment.

Keywords: Heavy metals; radionuclides; metal-organic frameworks; adsorption; photocatalytic reduction; pollution remediation

1. Introduction

In the past decades, contamination with heavy metals and organic pollutants has attracted increasing attention at a global scale due to their adverse health effects to human and aquatic organisms (Elzwayie et al., 2017; Fu et al., 2017; Schwarzenbach et al., 2010; Zou et al., 2016a; Ren et al., 2018a, 2018b, 2018c). Examples of the heavy metals include arsenic (As), lead (Pb), mercury (Hg), cadmium (Cd) and chromium (Cr), which have been found in concentrations ranging from ng/L to mg/L in surface water and industrial wastewater (Fu et al., 2017; Kim et al., 2013; Liu et al., 2017a; Singh et al., 2015; Smith and Steinmaus, 2009). Heavy metals have potential to induce acute and chronic toxicity (e.g., oxidative stress), developmental and reproductive toxicity, genotoxicity, and carcinogenicity on aquatic biota (Fu et al., 2017; Villaescusa and Bollinger, 2008; Wu et al., 2016a; Zhitkovich, 2011). Pb(II) released from pipe corrosion worldwide have recently apprehended serious concern (Abokifa and Biswas, 2017; Delile et al., 2016; Deshommes et al., 2016; Laidlaw et al., 2016; Masters et al., 2016; Pieper et al., 2017). Another great environmental concern emerges with the development of nuclear power, which produces and releases the radionuclides in natural waters (e.g., ^{235}U , ^{79}Se , ^{99}Tc , ^{137}Cs , and ^{90}Sr) (Ding et al., 2016; Little et al., 2016; Sheng et al., 2017; Steinhauser, 2014). Hence, a variety of removal techniques have been investigated. These techniques include physical adsorption by different kinds of adsorbents (e.g., carbon-based materials and metal oxides) and membrane-based filtration as well as photocatalytic redox processes to efficiently recover these heavy metals and radionuclides from the water (Carboni et al., 2013; Ding et al., 2016; Fu and Wang, 2011; Howarth et al., 2015; Hua et al., 2012; Huang et al., 2014; Kim et al., 2013; Liu et al., 2017a; Ma et al., 2016; Singh et al., 2015; Vellingiri et al., 2018; Vilela et al., 2016; Yu et al., 2015; Zou et al., 2016a).

Recently, a growing interest is on the development and application of inorganic-organic hybrid porous materials, known as metal-organic frameworks (MOFs) (Bosch et al., 2017; Dhakshinamoorthy et al., 2018; Furukawa et al., 2013; Julien et al., 2017; Lin et al., 2014; Liu et al., 2017b; Qin et al., 2016; Shen et al., 2018; Zhou and Kitagawa, 2014). These synthetic solid materials are self-assembled through strong coordination bonds between the metal-containing units and organic linkers to produce the open crystalline networks with ultrahigh and permanent porosity (Cao et al., 2017; Feng et al., 2015b; Qin et al., 2016; Xie et al., 2017; Yuan et al., 2017b). In the chemical synthesis of MOFs, the bottom-up method (i.e., direct mixing of metal ions and organic ligands for *in situ* reactions) was commonly applied to grow the oriented crystals of MOFs. In this approach, different kinds of techniques were used, which include hydrothermal, solvothermal, electrochemical, mechanochemical, microwave, layer-by-layer growth, and high-throughput synthesis (Furukawa et al., 2013; Zhou and Kitagawa, 2014). This strategy can generally be classified into two categories: direct MOFs synthesis in nonaqueous or aqueous media and mixing the MOFs precursors at certain ratio in mixed non-aqueous/aqueous systems. Depending on the metal ions and/or clusters and organic ligands (e.g., carboxylates, phosphonates, cyano and pyridyl), MOFs have shown high flexibility in tuning their structures and properties (Chang et al., 2015; Furukawa et al., 2013; Yuan et al., 2015, 2016; Zhou and Kitagawa, 2014). To date, more than 20,000 different kinds of MOFs have been prepared and characterized, and widely applied in gas storage, luminescence, sensing, chemical catalysis, energy generation, biomedical imaging, environmental remediation, and so forth (Cao et al., 2017; Chang et al., 2015; Chen et al., 2014, 2017; Decoste and Peterson, 2014; Dhakshinamoorthy et al., 2018; Feng et al., 2015a; Hu et al., 2017; Julien et al., 2017; Li et al., 2009; Lin et al., 2014; Qin et al., 2016; Riccò

et al., 2018; Xie et al., 2017; Zhang and Lin, 2014; Zhang et al., 2018; Zhao et al., 2014; Cheng et al., 2018).

In the past decades, one of the advancements in the chemistry of MOF is their stability in water medium. The water-stable MOFs have shown their applications in water treatment. Owing to the exceptional porosity and high surface area, water-stable MOFs can adsorb toxic pollutants from air and water (Ahmed and Jhung, 2017; Decoste and Peterson, 2014; Hasan and Jhung, 2015; Khan and Jhung, 2017; Seo et al., 2016; Wen et al., 2018; Kobielska et al., 2018; Khan et al., 2013), catalytic removal of heavy metals and organic pollutants stemming from the unusual light harvesting and electron transfer of MOFs (Liu et al., 2017b; Wang et al., 2014, 2016a, 2016b; Zhang and Lin, 2014), and the improvement of membrane-based separations (Furukawa et al., 2013; Lin et al., 2014; Zhou and Kitagawa, 2014). In addition, some other composites such as carbon nanotubes, graphene, quantum dots, metal nanoparticles and metal oxides, have been applied for fabricating water-stable MOF-based nanoparticles, which exhibited significantly improved properties than MOFs alone (Chen et al., 2017; Falcaro et al., 2016). Many examples of applications of water-stable MOFs demonstrated their potentials as the green and recyclable materials to reduce the environmental risks of various contaminants.

Variation of different species of representative heavy metals and radionuclide (As(III), As(V), Pb(II), Hg(II), Cd(II), U(VI), Cr(III), and Cr(VI)) with solution pH is shown in Fig. 1a-h. Generally, solution pH alters the speciation (or charges of metal ions in water), which further affect the interactions between the dominated metal species and the organic linkers or metal-containing units of MOFs. For example, As(V) has a total of four existing forms as H_3AsO_4 , H_2AsO_4^- , HAsO_4^{2-} and AsO_4^{3-} , which dominate under the pH ranges of < 2.0 , 3.0-6.0, 7.0-11.0 and > 12.0 , respectively (Fig. 1b). Unlike the neutral form of As(V), three latter species are more susceptible

to be adsorbed by the cationic MOFs via electrostatic attraction. Therefore, the understanding on the existing speciation of different metal species could facilitate the functional design and modifications of water-stable MOFs for their effective recovery from aqueous phase.

<Fig. 1>

In the present paper, we present a systematical review of existing literature regarding the application of environmentally friendly water-stable MOFs and MOF-based composites for aqueous removal (adsorptive elimination and/or chemical transformation) of both heavy metal ions and radionuclides. A wide range of heavy metal species (e.g., As(III)/As(V), Pb(II), Hg(II), Cd(II), Cu(II) and Cr(III)/Cr(VI)) and radionuclides (e.g., U(VI), Se(IV)/Se(VI) and Tc(VII)) of greatest concern are chosen to demonstrate capturing of the target pollutants by water-stable MOFs.

2. Water stability of MOFs

Water stability of the porous materials is the prerequisite for their successful application to remove heavy metal ions and radionuclides in water (Burtch et al., 2014; Wang et al., 2016a). The water-stable MOFs should preserve their X-ray diffraction (PXRD) pattern and Brunauer–Emmett–Teller (BET) surface area after water treatments. Metal-ligand coordination bonds are the ‘weakest’ point in MOFs. Stability of MOFs in water is highly related to the strength of coordination bonds (Canivet et al., 2014). The interaction between water and MOFs can be considered as the competing coordination to metal ions/metal nodes between water molecule and organic linkers (Burtch et al., 2014). If the metal-organic coordination bond is strong enough, it is hard for water molecule to substitute the existing bond. Therefore, the whole MOFs show good water stability. The strength of the metal–ligand bonds also illustrates the fundamental of stability and determines the thermodynamic stability of MOFs (Burtch et al., 2014; Canivet et al., 2014; Feng et al., 2014). There are many other factors affecting the water stability, which include

crystallinity, metal-ligand coordination geometry, porosity, and pore surface hydrophobicity. The operating conditions like temperature and pH also need to be considered when evaluating the stability of MOFs in water. Overall, many factors stated above determine the stability of MOFs in water (Burtch et al., 2014; Canivet et al., 2014).

According to the hard/soft acid/base (HSAB) principle, strong coordination bonds are formed between hard acid vs hard base, and soft acid vs soft base. Carboxylate-based ligands are regarded as hard bases, so water-stable MOFs can be formed together with hard acid metal ions such as Cr^{3+} , Al^{3+} , Fe^{3+} , and Zr^{4+} . In early works, some representative MOFs with remarkable stability in water include MIL series (MIL stands for Material Institut Lavoisier and examples are MIL-53 (Serre et al., 2002), MIL-100 (Férey et al., 2004) and MIL-101 (Férey et al., 2005) and UiO series (UiO stands for University of Oslo and examples are UiO-66, UiO-67, and UiO-68). Another type of stable MOFs is assembled by soft base azolate ligands (including imidazoles, pyrazoles, triazoles, and tetrazoles) and soft acid metal ions (such as Zn^{2+} , Cu^{2+} , Ni^{2+} , Mn^{2+} and Ag^+). The most representative examples in this category are the zeolitic imidazolate frameworks (ZIFs), which is constructed by Zn^{2+} and imidazolate linkers (Park et al., 2006). In recent years, triazole and pyrazolate-based MOFs have been synthesized using Ni^{2+} , Co^{2+} , Cu^{2+} , and other transition metal ions, which have shown good stability in water and even in strong basic environments (Bosch et al., 2017; Chang et al., 2015; Lin et al., 2014; Zhou and Kitagawa, 2014).

3. Aqueous capture of As(III) and As(V)

In the past few years, MOFs and MOF-based composites have been increasingly suggested as the excellent adsorbents for removal of As(III) and As(V) from water (Audu et al., 2016; Cai et al., 2016; Folens et al., 2016; Huo et al., 2018; Jian et al., 2015, 2016; Li et al., 2014a, 2014b,

2015; Liu et al., 2015; Luo et al., 2017; Nasir et al., 2018; Vu et al., 2015; Wang et al., 2015, 2016b; Wu et al., 2014; Yang and Yin, 2017; Zhu et al., 2012; Zou et al., 2016b). Among these studies, Fe-based MOFs (e.g., MIL-53(Fe) and MIL-100(Fe)), ZIF-8 and UiO-66 were the most commonly used adsorbents. The maximum adsorption capacity (q_{\max}) of these components was found in the range from 49.49 mg/g (ZIF-8) to 143.6 mg/g (CoFe₂O₄/MIL-100(Fe)) for As(III) and from 12.29 mg/g (Fe-BTC) to 303 mg/g (UiO-66) for As(V), respectively (Table 1). Generally, studies on the adsorption kinetics and isotherms of As species indicated that the adsorption processes were fitted well with the pseudo-second-order kinetic model and Langmuir adsorption model (Cai et al., 2016; Folens et al., 2016; Huo et al., 2018; Jian et al., 2015, 2016; Li et al., 2014a, 2014b, 2015; Liu et al., 2015; Vu et al., 2015; Wang et al., 2015; Yang and Yin, 2017; Zhu et al., 2012). The adsorptive elimination of As species was more likely a homogeneous monolayer adsorption that occurred at the interface of catalysts/water with no interaction between the adsorbed species (Folens et al., 2016; Zhu et al., 2012).

More recently, the adsorption isotherms of As(III) and As(V) by CoFe₂O₄/MIL-100(Fe) were fitted with the Freundlich and Langmuir models, respectively (Yang and Yin, 2017). Further investigations suggested the spontaneous characteristics of these adsorption processes; demonstrated by the negative values of ΔG (Yang and Yin, 2017; Zhu et al., 2012). In addition, these materials showed superior stability and reusability to remove As(III) and As(V) from water even after several recycles (Li et al., 2014a, 2015; Liu et al., 2015; Zhu et al., 2012). In cases of slightly reduced adsorptive performance, the leakage of some active metal species and/or organic linkers into aqueous solutions may be happening (Li et al., 2014a; Liu et al., 2015). The adsorption of As species using these adsorbents was commonly shown to be unaffected significantly by some coexisting ions (e.g., Ca²⁺, Mg²⁺, SO₄²⁻, CO₃²⁻, Cl⁻ and NO₃⁻), natural organic matters, and water

matrices (e.g., groundwater and surface water) (Cai et al., 2016; Folens et al., 2016; Li et al., 2014a, 2014b; Liu et al., 2015; Wang et al., 2015; Yang and Yin, 2017). These findings suggested that these water-stable MOFs and MOF-based composites could be used as the efficient, selective, and stable adsorbents for aqueous removal of As residues from real water and wastewater.

<Table 1>

Recent studies suggested that structural and functionalized design of MOFs could significantly affect the adsorptive performance of As species from water (Audu et al., 2016; Wu et al., 2014). As shown in Fig. 2a, ZIF-8 exhibited the better adsorption capacity (50.50 mg/g) of As(V) than active carbon (3 mg/g) and zeolite (13.92 mg/L). This phenomenon may be attributed to the open frameworks of ZIF-8 and its characteristic composition with abundant external active sites (Zn-OH) formed by dissociative adsorption of water, which could bind As(V) species more effectively (Wu et al., 2014). Notably, more significant enhancements on As(V) adsorption were found by adjusting the ratios of co-templates (cetyltrimethylammonium bromide and amino acid L-histidine), and the q_{\max} value of 90.92 mg/g was observed for H-ZIF-8-14. More recently, Audu et al. (2016) also reported some significantly improved As(III) adsorption profiles by thiolated UiO-66 compared to their non-functionalized analogues, further demonstrating the important role of the organic linkers for capturing As(III) (Fig. 2b). Similarly, Shen et al. (2015) studied the photocatalytic oxidation of As(III) over UiO-66 and three different functionalized UiO-66-X catalysts (X = NH₂, NO₂ and Br). The apparent first-order rate constants suggested that the UiO-66-NH₂ had the highest catalytic performance, followed by UiO-66, UiO-66-Br and UiO-66-NO₂. These results may be attributed to the higher electron density of organic ligands by introducing electron donor (-NH₂), which can improve the transfer of photo-induced charge carriers in order to enhance the photocatalytic capability for As(III) oxidation (Shen et al., 2015).

<Fig. 2>

The adsorption mechanisms of As(III) and/or As(V) by MOFs and MOF-based composites involved the important role of hydroxyl groups on the surface of MOFs (Audu et al., 2016; Jian et al., 2015; Li et al., 2014a; Liu et al., 2015; Wang et al., 2015; Yang and Yin, 2017). Recently, Jian et al. (2015) proposed two steps for removing As species from water: (1) water molecules adsorbed on ZIF-8 interacted with zinc atom and initiate protonated reactions with certain surface groups (e.g., C=N⁻ and C-NH⁻) to produce active sites, including Zn-OH, C=NH⁺ and C-NH₂⁺; (2) electrostatic attraction occurred between these positive sites and negative arsenate species to form some inner-sphere complexes (Fig. 2c). Similar mechanisms were also reported to adsorb trace amount of As(V) by ZIF-8 (Li et al., 2014a). As(III) removal by cubic, leaf-shaped and dodecahedral ZIF-8 (Liu et al., 2015), as well as selective adsorption of As(III)/As(V) by CoFe₂O₄/MIL-100(Fe) have also been reported (Yang and Yin, 2017). Interestingly, a dual capture of As(V) and As(III) was reported via the application of UiO-66 and its analogues, which represented a promising adsorptive strategy for effective elimination of the mixed As pollution (Audu et al., 2016). It is noteworthy to mention that the introduction of thiol-containing BDC linkers could strongly coordinate As(III) by their -SH groups, while Zr₆O₄(OH)₄ cluster nodes could bind with As(V) oxyanions through hydroxyl exchange procedure (Fig. 2d) (Audu et al., 2016). Therefore, more selective and efficient removal of these two As species could be achieved simultaneously.

4. Aqueous capture of Pb(II) and Hg(II)

In light of detection of Pb(II) in a wide range of waters, several studies have been carried out on its adsorption onto ultrahigh porosity and high surface area of water-stable MOFs and MOF-based composites (Abney et al., 2014a; Alqadami et al., 2018; Babazadeh et al., 2015; Ghorbani-

Kalhor et al., 2014; Ghorbani-Kalhor, 2016; Hassanpour et al., 2015; Huang et al., 2018; Jamali et al., 2016; Luo et al., 2015; Nalaparaju and Jiang, 2012; Peng et al., 2018; Ricco et al., 2015; Salarian et al., 2014; Saleem et al., 2016; Shi et al., 2018; Taghizadeh et al., 2013; Tahmasebi et al., 2015; Tokalioglu et al., 2017; Wang et al., 2017; Yin et al., 2016, 2018; Yu et al., 2017; Zhang et al., 2016b). Among them, most literature just focused on the application of these adsorbents for solid-phase extraction and pre-concentration of Pb(II) in different environmental samples (Babazadeh et al., 2015; Ghorbani-Kalhor et al., 2014; Jamali et al., 2016; Salarian et al., 2014; Sohrabi et al., 2013; Taghizadeh et al., 2013; Tahmasebi et al., 2015; Tokalioglu et al., 2017). The reported q_{\max} values of Pb(II) were determined in range from 3.05 mg/g (Dy-MOF) to 1348.42 mg/g (ZIF-67) (Table 2). In recent pollution remediation studies of Pb(II), aqueous adsorption of Pb(II) onto MOFs and MOF-based composites was fitted well with the pseudo-second-order kinetic model and Langmuir isotherm model (Figs. 3a and 3b). These two models suggested the dominating chemical adsorption and monolayer adsorption process of Pb(II) by the adsorbents, respectively (Luo et al., 2015; Saleem et al., 2016). Additionally, Luo et al. (2015) reported the introduction of $-\text{NH}_2$ groups in ethylenediamine (ED) to the unsaturated Cr metal centers by strong coordination bonds. The functionalized ED-MIL-101(Cr) exhibited the superior selectivity and good regeneration capability for adsorbing Pb(II) (Figs. 3c and 3d). The selectivity coefficients between Pb(II) and four other metals (Cu(II), Zn(II), Co(II) and Ni(II)) were 6.92, 24.02, 15.69 and 14.53, respectively. Similar phenomena were also reported for aqueous capturing of Pb(II) and Cd(II) by NH_2 -functionalized Zr-MOFs, which exhibited the high adsorption capacity of 166.74 mg/g and 177.35 mg/g, respectively (Wang et al., 2017). Notably, the modified MOFs could achieve almost 100% removal of Pb(II) (10 mg/L) after 120 min. The mechanistic analysis also showed the coordination interactions of N in the amino group of Zr-MOFs with Pb(II) and

Cd(II) (Wang et al., 2017), which was further confirmed by FT-IR and X-ray photoelectron spectroscopy (XPS) survey. Recently, Yu et al. (2017) developed a novel Zn(II)-based MOF by introducing the negatively charged O⁻ groups into the pores of MOFs for Pb(II) capture. The ultrahigh adsorption capacity (616.64 mg/g) was derived from the strong electrostatic and coordination interactions between the O⁻ groups of MOFs and Pb(II) (Fig. 3e).

<Table 2>

<Fig. 3>

Regarding aqueous elimination of Hg(II) species, an increasing number of studies have also been performed by water-stable MOFs and MOF-based composites (Abbasi et al., 2015; Abney et al., 2014a; Bhattacharjee et al., 2015; Fang et al., 2010; Ghorbani-Kalhor et al., 2015; Halder et al., 2017; Han et al., 2016; Huang et al., 2016; Liu et al., 2014; Luo et al., 2015, 2016; Mon et al., 2016; Peng et al., 2018; Saleem et al., 2016; Wang et al., 2017; Wu et al., 2016b; Yee et al., 2013; Zhang et al., 2016a, 2016b). As shown in Table 2, some high q_{\max} values of Hg(II) were reported (e.g., 836.7 mg/g for JUC-62 and 769 mg/g for UiO-66NHC(S)NHMe). The pseudo-second-order kinetic model and Langmuir isotherm model were suggested for trapping Hg(II) by these MOF adsorbents; indicating the monolayer chemisorption onto a homogeneous surface (Huang et al., 2016; Luo et al., 2015, 2016; Saleem et al., 2016; Wu et al., 2016b). Similar to Pb(II) capturing, recent studies also showed certain functionalized groups (e.g., hydroxyl, acylamide and thiol) in the channels of MOFs as the responsible binding sites for efficient coordinating and adsorbing Hg(II) (Liu et al., 2014; Luo et al., 2015). For example, Liu et al. (2014) reported the synthesis of Cr-MIL-101-AS by tandem post-synthetic modifications for Hg(II) capture. The strong coordination between -SH and Hg(II) contributed to the excellent removal efficiency (99.3%) for Hg(II) (10 mg/L) (Fig. 4a). Similar results were also observed by the water-stable BioMOF with methionine groups in the hexagonal channels, which captured 99.95% Hg(II) (10 mg/L), and the

residual concentration of 5 ppb was well below the permissible limit in portable water (Mon et al., 2016). Additionally, the superior adsorption performance of MOFs (e.g., Cr-MIL-101-AS) has also been observed for the ultra-low level of Hg(II) (ng/L- μ g/L) (Liu et al., 2014; Luo et al., 2016). Luo et al. (2016) reported the application of MIL-101-Thymine for removing trace Hg(II) (45 ng/L-4.7 μ g/L) in real water and wastewater. The extremely high removal efficiency (98.8%-100%) showed the high potential of MOF materials for recovering Hg(II) species in natural waters. Mechanistic analysis suggested that Hg(II) strongly two-coordinated with N atoms of the thymine ligands of MOFs (Fig. 4b), confirmed by XPS analysis. In addition, MIL-101-Thymine presented excellent selectivity to Hg(II) in presence of multiple metal ions (e.g., Pb^{2+} , Cd^{2+} , Co^{2+} , Ni^{2+} and Cu^{2+}) due to the highly characteristic formation of T-Hg(II)-T groups. The selective coefficient of 947.34 was extremely high.

<Fig. 4>

5. Aqueous capture of Cr species (Cr(III) and Cr(VI))

5.1. Adsorption

More recently, aqueous adsorption by MOFs and MOF-based composites has been widely investigated and demonstrated as an effective and feasible treatment for removing Cr species (Aboutorabi et al., 2016; Custelcean et al., 2012; Desai et al., 2016; Fei et al., 2011, 2013; Fu et al., 2015; Li et al., 2013, 2015, 2017; Lupa et al., 2017; Nasrollahpour and Moradi, 2017; Niknam Shahrak et al., 2017; Niu et al., 2017; Rapti et al., 2016a, 2016b; Saleem et al., 2016; Shi et al., 2012; Tahmasebi et al., 2015; Wu et al., 2017; Zhang et al., 2015; Zhu et al., 2017a). Almost all these investigations focused on the adsorption of Cr(VI), with the q_{max} values ranging from 0.15 mg/g (ZIF-8) to 1709.2 mg/g (1D Fe-gallic acid). The highest value of 127 mg/g was reported for Cr(III) adsorption by TMU-4 (Table 3). Similar to the adsorption of above heavy metal ions,

aqueous adsorption of Cr(III) and/or Cr(VI) by water-stable MOFs was generally fitted with the pseudo-second-order kinetic model and Langmuir isotherm model (Aboutorabi et al., 2016; Falcaro et al., 2016; Li et al., 2015, 2017; Lupa et al., 2017; Nasrollahpour and Moradi, 2017; Niu et al., 2017; Saleem et al., 2016; Wu et al., 2017; Zhu et al., 2017a). Based on the adsorption thermodynamics, the spontaneity and endothermic nature of these removal processes were individually suggested by the negative values of Gibbs free energy change (ΔG°) and positive values of standard enthalpy change (ΔH°). (Aboutorabi et al., 2016; Nasrollahpour and Moradi, 2017; Wu et al., 2017). Additionally, these MOFs exhibited the excellent selectivity in the presence of high concentrations of disturbing ions (e.g., Cl⁻, Br⁻, NO₃⁻, SO₄²⁻, I⁻ and F⁻) (Aboutorabi et al., 2016; Fei et al., 2013; Wu et al., 2017; Zhang et al., 2015) and superior reusability after several cycles (Aboutorabi et al., 2016; Fu et al., 2015; Li et al., 2015; Niu et al., 2017; Zhu et al., 2017a).

<Table 3>

It was demonstrated that the single-crystal-to-single-crystal (SC-SC) transformation via anion exchange contributed to most of the adsorptive processes of Cr(VI) by water-stable MOFs. Examples include SLUG-21 (Fei et al., 2011), {[Cu₄(μ₃-OH)₂(mtrb)₂(1,4-bda)₂]Br₂·6H₂O}_n (Lv et al., 2017), {[Dy₂Zn(BPDC)₃(H₂O)₄](ClO₄)₂·10H₂O}_n (Shi et al., 2012), Zn_{0.5}Co_{0.5}-SLUG-35 (Fei et al., 2013), ZJU-101 (Zhang et al., 2015), {[Ni₂(L)₃-(SO₄)(H₂O)₃]·(SO₄)·x(G)}_n (Desai et al., 2016), MOR-1-HA (Rapti et al., 2016b), {[Ag₈(tz)₆](NO₃)₂·6H₂O}_n (Li et al., 2017), ABT·2ClO₄ (Li et al., 2013) and FIR-53 (Fu et al., 2015). Li et al. (2013) reported the use of ABT·2ClO₄ (a cation MOF) for aqueous exchanging of Cr(VI). Based on the changes of UV/Vis spectra, efficient adsorptive removal of Cr(VI) was observed by ABT·2ClO₄ after 48 h (Fig. 5a). Further FT-IR analysis suggested the SC-SC adsorptive mechanisms through the formation of ABT·Cr₂O₇ from the interactions between ABT·2ClO₄ and Cr(VI) (Fig. 5b). Similarly, Fu et al. (2015) reported that the Cr₂O₇²⁻ could fill into the channels of the frameworks of FIR-53, and the initial NO₃⁻ was

exchanged by the guest anions (Fig. 5c). The results from single-crystal X-ray diffraction and the observed weak C-H...O interactions validated this mechanism.

<Fig. 5>

In addition to the SC-SC mechanism, the adsorption-reduction processes of Cr(VI) have also been reported by the ZIF-based adsorbents such as ZIF-67 and magnetic polydopamine@ZIF-8 (MP@ZIF-8) (Li et al., 2015; Zhu et al., 2017a). Similar to the adsorptive removal of As species, Li et al. (2015) proposed that the uncoordinated Co(II) in ZIF-67 microcrystals could react with water to generate the active Co–OH group, which could adsorb Cr(VI) species by ion exchange. Subsequently, the electron donated framework could partly act as the reductant to transform Cr(VI) to Cr(III) in water (Fig. 5d). The relatively high Cr(VI) concentration gradient and electrostatic interaction could also facilitate the mass transfer of Cr(VI) onto the surface of ZIF-67, thus effectively reducing the concentration and pollution of Cr(VI) in water. More recently, Zhu et al. (2017a) also suggested that the active sites (e.g., Zn–OH and protonated N atom groups), generated by the interaction of ZIF-8 and water, could efficiently adsorb Cr(VI), which could be partially reduced to Cr(III) by some amine groups (e.g., =N– and –NH– groups) of imidazolate ligands. Overall, the adsorptive processes of aqueous Cr(VI) by MOFs involved multi-steps, and the SC-SC transformation and combined adsorption-reduction contributed to two main adsorptive mechanisms in water.

5.2. Reduction

5.2.1. Photocatalytic reduction of Cr(VI)

MOFs have semiconductor-like characteristics under UV/Vis light irradiation because the organic linkers harvest light to activate the metal sites by charge transition from linkers to metal-oxo clusters (Dhakshinamoorthy et al., 2016, 2017; Wang, et al., 2014). Subsequently, the photo-

generated electrons and holes by the excited MOFs initiate effective heterogeneous photo-redox processes for transforming organic pollutants and heavy metals (Canlas et al., 2012; Zhang and Lin, 2014). The superior adsorption of MOFs, derived from the desirable structure and high surface area, facilitates the rapid accumulation of target molecules into the nano-reactors (Wang et al., 2016b; Zeng et al., 2015). Therefore, efficient removal of environmental contaminants is achieved by using the MOF-catalyzed photochemical treatments.

In the past few years, the application of water-stable MOFs and MOF-based composites to carry out photocatalytic Cr(VI) reduction has been studied. The visible light has been extensively investigated to test feasibility of this technology in real water environment (Huang et al., 2017; Liang et al., 2015a, 2015b, 2015c, 2015d, 2015e; Shen et al., 2013a, 2013b, 2014; Shi et al., 2015; Wang et al., 2015a, 2015b; Zhao et al., 2017). As shown in Table 4, Fe-based MOFs (e.g., MIL-53(Fe), MIL-100(Fe) and MIL-101(Fe)) have exhibited superior catalytic performance for reducing Cr(VI) under visible light irradiation. Notably, NH₂-functionalized MOFs such as MIL-68(In), MIL-125(Ti), MIL-68B(Fe) and UiO-66 greatly improved the photocatalytic activity of their non-functionalized forms (Liang et al., 2015e; Shen et al., 2013a; Shi et al., 2015; Wang et al., 2015b). For example, only slight Cr(VI) reduction (< 20% after 60 min) was observed during visible light-driven photocatalytic treatment over MIL-88B(Fe) (Fig. 6a). Comparatively, NH₂-MIL-88B(Fe) showed the excellent catalytic ability, having complete reduction of Cr(VI) in 45 min (Shi et al., 2015). In addition, some hybrid photocatalysts of MOFs with semiconductors (e.g., Me_xS_y and ZnO) or conductors (e.g., Pd and RGO) have been demonstrated to enhance the photocatalytic performance significantly (Liang et al., 2015d; Shen et al., 2013b, 2014; Wang et al., 2015a, 2016b). Recently, Liang et al. (2015b) reported the immobilization of three highly dispersed noble-metal nanoparticles (Au, Pd and Pt) on MIL-100(Fe), and used them as the visible-

light photocatalysts for reducing Cr(VI) in water. The irradiation time for achieving complete reduction of aqueous Cr(VI) was 8, 16, 20 and 24 min for Pt@MIL-100(Fe), Pd@MIL-100(Fe), Au@MIL-100(Fe) and MIL-100(Fe), respectively (Fig. 6b). This phenomenon suggested the important role of these noble metals during photocatalytic reduction of Cr(VI). These MOF-based nanocatalysts also presented the stable and reusable catalytic performance after four recycling times (Figs. 6c and 6d). This indicates promising use of MOF-based nanocatalysts in successive treatments of the Cr(VI)-polluted water and wastewater.

<Table 4>

<Fig. 6>

Based on the above studies, the photocatalytic mechanisms of Cr(VI) reduction by MOFs have been proposed. In a recent review, Wang et al. (2016b) summarized that the introduction of $-NH_2$ group and conductor composites (e.g., Me_xS_y , ZnO, Pd and RGO) to improve greatly the electron-hole pair separation and the photo-generated electron transfer from the organic ligands to metal-oxo clusters, thus facilitating the rapid Cr(VI) reduction. For example, Shi et al. (2015) studied the photocatalytic reductive processes of Cr(VI) by NH_2 -MIL-88B(Fe) and proposed the dual excitation pathways: (1) $Fe_3-\mu_3$ -oxo clusters could be directly excited under visible light irradiation to produce the reactive electron for Cr(VI) reduction; and (2) NH_2 -functionalized organic ligands could also be excited, and photo-generated electron was transferred to the $Fe_3-\mu_3$ -oxo clusters for performing reductive reactions (Fig. 6e). Also, the $-NH_2$ group could accelerate the electron transfer and reduce the recombination of electron-hole pairs. Hence, the significantly enhanced photocatalytic performance was achieved. More recently, similar catalytic mechanisms were also reported by incorporating g- C_3N_4 on the surface of MIL-53(Fe), in which the efficiency of electron migration and the separation of photo-induced electron and hole pairs could be

remarkably promoted (Fig. 6f) (Huang et al., 2017). The proposed reactions are shown below (Eqs. 1-4):



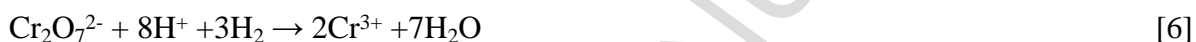
5.2.2. Reductive transformation of Cr(VI) by formic acid

Recently, two studies investigated the reductive conversion of Cr(VI) to Cr(III) using formic acid, catalyzed by metal nanoparticles immobilized MOFs (Table 4) (Trivedi et al., 2016; Yadav and Xu, 2013). Yadav and Xu (2013) synthesized four different kinds of M@MIL-101 composites (M = Pt, Pd, Au and Rh) by the double solvents method, and the catalytic reduction of Cr(VI) by excess of formic acid in water was carried out. No significant conversion of Cr(VI) was found with the additions of 2 wt% Au@MIL-101 and Rh@MIL-101. Comparatively, 2 wt% Pt@MIL-101 and Pd@MIL-101 showed highly catalytic performance in which complete conversion of Cr(VI) was observed within 40 and 210 min, respectively (Fig. 7a). The possible reason was suggested to be the formation of reactive metal-formate intermediate by the adsorbed formic acid on the surface of Pt or Pd nanoparticles, which catalyzed the reduction of Cr(VI) efficiently (Yadav and Xu, 2013).

<Fig. 7>

More recently, Trivedi et al. (2016) also reported the excellent catalytic capability of bimetallic Pd-Cu/MIL-101 nanocomposites to convert Cr(VI) by formic acid. Reduction of Cr(VI) by the bimetallic nanocomposites was much faster than Pd-Cu nanocrystals by a factor of 3-5 times. A 2 wt% Pd_{0.5}Cu_{0.5}@MIL-101 showed the higher catalytic performance than some other ratios of

Pd and Cu in the MOF-based catalysts (Fig. 7b). The efficient reduction of Cr(VI) was attributed to the nascent H₂, which was generated from the decomposition of formic acid adsorbed on the surface of catalysts (Fig. 7c and Eqs. 5-6) (Akiya and Savage, 1998; Trivedi et al., 2016; Yalfani et al., 2008). In addition, 2 wt% Pd_{0.5}-Cu_{0.5}@MIL-101 also exhibited the high stability and superior reusability during catalytic reduction of Cr(VI) in five successive runs (Fig. 7d). Formic acid-mediated reductive processes in combination with hybrid MOFs-supported metal nanocomposites could be employed as the green and efficient methods to treat Cr(VI)-polluted water and wastewater.



6. Aqueous capture of some other heavy metal ions

In addition to the above heavy metals, water-stable MOFs and MOF-based composites have also been used in water to remove some other species, such as Cd(II) (Abbasi et al., 2015; Abney et al., 2014a; Babazadeh et al., 2015; Fang et al., 2010; Ghorbani-Kalhor, 2016; Roushani et al., 2017; Saleem et al., 2016; Sohrabi et al., 2013; Taghizadeh et al., 2013; Tahmasebi et al., 2015; Wang et al., 2017; Zhang, et al., 2016b), Cu(II) (Huang et al., 2018; Jamali et al., 2016; Tahmasebi et al., 2015; Wang et al., 2014, 2017), Ni(II) (Ghorbani-Kalhor, 2016; Taghizadeh et al., 2013), Zn(II) (Babazadeh et al., 2015; Taghizadeh et al., 2013), Co(II) (Fang et al., 2010; Tahmasebi et al., 2015; Yuan et al., 2017a), and Mn(VII) (Fei et al., 2011). As shown in Table 4, the q_{max} values of these heavy metal ions have been determined as 210 mg/g (Fe₃O₄@TAR), 617.51 mg/g (ZIF-67), 196 mg/g (Fe₃O₄@TAR), 206 mg/g (MOF-DHz), 256 mg/g (UiO-66-Schiff), and 292 mg/g (SLUG-21), respectively. Among these studies, Fei et al. (2011) reported the application of SLUG-

21, an Ag(I)-based cationic MOF, for removing Mn(VII) oxyanions in water. The adsorption capability (292 mg/g) was five times more than that of conventional adsorbents (e.g., layer double hydroxides). Furthermore, this cationic material also showed superior selectivity for capturing three oxo-anion metal pollutants (Mn(VII), Re(VII) and Cr(VI)) even in presence of 100-fold excess of NO_3^- and CO_3^{2-} in water. The mechanism was proposed to occur through the SC-SC transformation rather than the equilibrium-driven anion exchange. The target Mn(VII) could be trapped into the new crystal structure permanently. Additionally, similar to the adsorption of As(III)/As(V), Pb(II) and Hg(II) by MOFs, Yuan et al. (2017a) recently reported that Co(II) capturing by UiO-66-Schiff was spontaneous and endothermic. The adsorptive process followed the pseudo-second-order chemisorption and Langmuir isotherm model. This study applied the density functional theory (DFT) calculations and XPS analysis to demonstrate that the carboxyl oxygen and Schiff base nitrogen in the ligands of UiO-66-Schiff were the major binding sites for capturing Co(II).

A more recent study developed a versatile MOF-based trap via incorporation of ethylenediaminetetraacetic acid (EDTA) into highly robust MOF-808 (Fig. 8a) (Peng et al., 2018). This modified material showed excellent single-component adsorption efficiency (> 99%) non-specifically for removing 22 metal ions, belonging to category of hard acids, soft acids and borderline acids. Also, the adsorption of La(III), Pb(II) and Hg(II) by MOF-808-EDTA was fitted well with the pseudo-second-order kinetic model and Langmuir isotherm model. In terms of coexisting metal species in natural waters, this study found that the MOF-808-EDTA could capture 19 multifarious metal ions simultaneously and efficiently in multi-component systems. The strong chelation of heavy metals by EDTA ligands caused such high elimination efficiency (Fig. 8b). Further breakthrough experiments showed that these heavy metal ions at initial concentration of 5

mg/L can be almost completely removed in the fixed bed adsorption (Fig. 8c). The extremely low metal residues (0.01-1.9 $\mu\text{g/L}$) after water purification made this porous material as an innovative candidate in industrial set-up applications.

<Fig. 8>

Overall, water-stable MOFs and MOF-based materials have been commonly demonstrated as the promising composites for eliminating a wide range of heavy metal species in water efficiently. The adsorption mechanisms mainly include coordination interactions, hydrogen bonding, ion exchange, electrostatic interaction, Lewis acid-base interaction, and combined adsorption-reduction (Fig. 9). Among them, one or two mechanisms may be dominated and responsible for aqueous capture of certain heavy metal ions by these porous materials.

<Fig. 9>

7. Aqueous recovery of radionuclides by MOFs

As one of the most hazardous radionuclides in the water environment, U(VI) has attracted increasing attention for its recovery and pollution remediation (Bai et al., 2016; Feng et al., 2016; Kim et al., 2013; Lashley et al., 2016; Li et al., 2017; Ogden et al., 2017; Shao et al., 2016). Notably, MOFs and MOF-based composites have also been investigated extensively to capture U(VI) (Bai et al., 2015; Carboni et al., 2013; De Decker et al., 2017; Li et al., 2016, 2017; Liu et al., 2016, 2017a; Luo et al., 2016; Song et al., 2016; Wang et al., 2015; Xiong et al., 2016; Yang et al., 2013). To date, the q_{max} values were mostly reported in a range from 100 to 350 mg/g. The highest value of 350 mg/g was reported onto MIL-101-DETA (Table 5). Similar to the above metals, the adsorption of U(VI) by these adsorbents (e.g., MIL-101-Ship, MOF-3, UiO-66 and UiO-66-NH₂) was fitted well with the pseudo-second-order kinetic model and Langmuir isotherm model (Bai et al., 2015; Carboni et al., 2013; De Decker et al., 2017; Li et al., 2016, 2017; Liu et al., 2016, 2017a;

Luo et al., 2016; Wang et al., 2015; Yang et al., 2013). The spontaneous and endothermic characteristics of the chemisorption process were also suggested, based on the thermodynamic data (Wang et al., 2015).

<Table 5>

As a typical Lewis acid, U(VI) is known to be strongly coordinated with the hard bases such as amine donors and oxygen-containing groups (Liu et al., 2017a). More recently, Liu et al. (2017a) introduced a kind of luminescent mesoporous terbium(III)-based MOF material, equipped with abundant Lewis basic groups, for recovering U(VI). It was proposed that the amine groups were the main binding sites for efficient and preferential complexing U(VI). The excellent adsorptive performance was attributed to the amine donors-dominated inner-sphere coordination mechanism, demonstrated by the combined X-ray absorption spectroscopy and first principles simulation. Similarly, Bai et al. (2015) also prepared three different amino-functionalized MIL-101, and reported the highest q_{\max} value of 350 mg/g at pH \sim 5.5 for MIL-101-DETA, followed by MIL-101-ED, MIL-101-NH₂ and MIL-101 (Fig. 10a). This phenomenon was mainly attributed to more amounts of amine sites available in the pores of MIL-101-DETA for U(VI) coordination. Additionally, this MOF material also presented superior selectivity for U(VI) at pH 4.5 and 5.5, with the extremely stronger binding affinity for U(VI) ($>$ 6000 mL/g) than all other metal ions ($<$ 100 mL/g) (Fig. 10b).

<Fig. 10>

The introduction of more oxygen-containing groups into MOFs has also been demonstrated to enhance recovery of U(VI) species (Carboni et al., 2013; Li et al., 2016; Wang et al., 2015). Recently, Carboni et al. (2013) reported the inclusion of orthogonal phosphorylurea groups into UiO-68 network and used this material for adsorbing U(VI) in water. The strong coordination of U(VI) with the phosphoryl oxygen was proposed in a monodentate mode, contributing to the high

adsorption capacity ($q_{\max} = 217$ mg/g) (Fig. 10c). The carboxyl groups were also suggested as the effective contributors for capturing U(VI) (Li et al., 2016; Wang et al., 2015). Wang et al. (2015) reported the recovery of U(VI) using the acylamide- and carboxyl-functionalized MOFs. This material exhibited the ultrafast extraction performance of U(VI) from seawater, i.e., 0.53 mg/g from 1 L artificial seawater containing 6 ppb U(VI) in 1 min. The excellent extraction capability was due to the free standing carboxyl groups in the MOF channel (Figs. 10d and 10e), which could capture U(VI) efficiently through the formation of strong U–O coordination bond. Also, the regeneration ability of the adsorbed MOFs was evaluated by different elution solutions (i.e., 0.1 M HCl, 0.1 M HNO₃ and 0.1 M Na₂CO₃). Almost complete desorption of U(VI) was observed using 0.1 M Na₂CO₃ eluent (Fig. 10f). This suggests a great potential of this material for practical extracting and recovering U(VI) from natural waters.

Furthermore, water-stable MOFs (e.g., NU-1000 and UiO-66-HCl) have also been used to capture Se(IV)/Se(VI) in water (Custelcean et al., 2012; He et al., 2017; Howarth et al., 2015; Li et al., 2017). Especially, Howarth et al. (2015) recently compared the adsorption capability of seven different Zr-based MOFs, including UiO-66, UiO-66-NH₂, UiO-66-(NH₂)₂, UiO-66-(OH)₂, UiO-67, NU-1000 and NU-1000BA, for capturing Se species (Se(IV) and Se(VI)) from water. Among them, NU-1000 exhibited the highest uptake performance (90% for Se(IV) and 88% for Se(VI)) after exposure to 100 mg/L Se solution (Fig. 11a). Based on the Langmuir adsorption equation, the q_{\max} values were 95 mg/g and 85 mg/g for Se(IV) and Se(VI), respectively. Also, NU-1000 showed the excellent adsorption efficiency for low-concentration Se species (1000 ppb); 98% removal was noted within 5 min, which met the EPA standards for drinking water (< 50 ppb Se).

Mechanistic analysis suggested that both Se(IV) and Se(VI) were bound to the Zr_6 -node by replacing its terminal –OH groups, i.e., each Se anion bridges two Zr_6 -metal sites. This was further confirmed by the pair distribution function analysis of the X-ray scattering data (Fig. 11b). Additionally, a recent study reported that the adsorption capacity of Se(VI) species can be greatly enhanced by introducing more amounts of missing linker defects or cluster defects instead of longer organic linkers into Zr-based MOFs (Li et al., 2017). The reason was shown as the increasing pore size of MOFs and more defects as the binding sites for capturing Se(VI) via modulator synthetic strategy. The anion exchange adsorptive mechanism of Se(VI) species by different compensating ligands (HO^- , Cl^- , H_2O , $O_2C-CH_3^-$, $O_2C-CF_3^-$ or $O_2C-CHF_2^-$) of MOFs was also demonstrated by the combined experimental and theoretical methods.

<Fig. 11>

In addition to aqueous capture of U(VI) and Se(IV)/Se(VI) by water-stable MOFs, several studies also reported the adsorption of some other radionuclides such as Cs(I) (Aguila et al., 2016; Wang et al., 2015), Sr(II) (Abney et al., 2014b; Aguila et al., 2016), Th(IV) (Zhang, et al. 2017), Tc(VII) (Sheng et al., 2017), and Re(VII) (the nonradioactive surrogate) (Banerjee et al., 2016; Fei et al., 2011; Sheng et al., 2017; Zhu et al., 2017b). Wang et al. (2015) synthesized a 3D water-stable uranyl polycatenated porous framework material with high radiation-resistance. The batch adsorption experiments indicated that it could capture Cs(I) in a short contact time (20 min) with the q_{max} value of 145 mg/g. Also, the excellent selectivity for capturing Cs(I) (as high as 71.80%-93.50% removal) was also observed even in the presence of 5 or 20 mass equivalences of other competing cations (Li^+ , Na^+ , K^+ , Rb^+ , Mg^{2+} and Ca^{2+}).

Recently, UiO-66 and two carboxyl derivatives (UiO-66-COOH and UiO-66-(COOH)₂) were explored to capture Th(IV) in weak acidic solution (Zhang et al., 2017). It was noted that the introduction of carboxyl groups into UiO-66 could greatly increase the coordinative adsorption of

Th(IV), with the q_{\max} value of 350 mg/g and superior selectivity coefficient (> 18) for UiO-66-(COOH)₂. For Tc(VII), recent studies commonly used Re(VII) as its nonradioactive surrogate to assess the capture performance of the water-stable MOFs (Banerjee et al., 2016; Fei et al., 2011; Sheng et al., 2017; Zhu et al., 2017b). Notably, the high exchange capacity of 541 mg/g and 786 mg/g was individually reported for trapping Re(VII) in water by two cationic MOFs, i.e., SCU-100 (Sheng et al., 2017) and SBN (Zhu et al., 2017b). The single crystal X-ray diffraction suggested the selective coordination of Re(VII) to the open Ag⁺ sites of MOFs, forming strong Ag-O-Re bonds and hydrogen bonds and thus achieving the SC-SC transformation. Fig. 12A illustrated the anion exchange process of SBN via complete substitution of NO₃⁻ by Re(VII), which was further confirmed by the increase of two new peaks at 896 and 860 cm⁻¹ and the decreased peak at 1326 cm⁻¹ in the FT-IR spectra of the samples before and after Re(VII) capture (Fig. 12B) (Zhu et al., 2017b). Additionally, SBN presented the high adsorption selectivity for capturing Re(VII); complete elimination in the presence of other coexisting anions (e.g., H₂PO₄⁻, SO₄²⁻, CO₃²⁻, NO₃⁻, ClO₄⁻ and Cl⁻) (Fig. 12C).

<Fig. 12>

8. Regeneration of water-stable MOFs during removal of heavy metals and radionuclides

It is highly desirable to regenerate these porous materials for the practical application of water-stable MOFs in water treatment. Based on the literature, several methods are reported as the effective candidates for regenerating water-stable MOFs, mainly including the elution via acids (e.g., HCl and HNO₃) (Roushani et al., 2017; Bai et al., 2015; Yuan et al., 2017; Shahrak et al., 2017; Audu et al., 2016; Cai et al., 2016; Carboni et al., 2013; Zhang et al., 2017; Liang et al., 2015c, 2015d, 2015e; Yu et al., 2017; Wang et al., 2015; Liu et al., 2017), thiourea and acid (Luo et al., 2016; Li et al., 2014b), NaOH (Audu et al., 2016; Li et al., 2014a, 2015; Liu et al., 2015;

Nasir et al., 2018), Na_2CO_3 (Li et al., 2016; Yang et al., 2013; Wang et al., 2015) or K_2CO_3 (Shi et al., 2012), EDTA-2Na (Luo et al., 2015; Peng et al., 2018), Na_2EDS (Li et al., 2017) and ion-exchange triggers such as NO_3^- (Fu et al., 2015; Li et al., 2017; Sheng et al., 2017), SO_4^{2-} (Li et al., 2015) and Br^- (Lv et al., 2017). Depending on the types of MOFs and metal species, different methods could be used to enhance the desorption performance. It has been widely demonstrated that elution with HCl and HNO_3 could effectively regenerate most kinds of MOFs (e.g., ZIF-8 (Shahrak et al., 2017), UiO-66 (Audu et al., 2016; Zhang et al., 2017), TMU-16- NH_2 (Roushani et al., 2017), MIL-100(Fe) (Cai et al., 2016), MIL-68(In)- NH_2 (Liang et al., 2015e), MIL-125(Ti)- NH_2 (Wang et al., 2015). Song et al. (2016) investigated the regeneration of four different 3D-MOFs (1-H, 1-OH, 1- NH_2 and 1- NO_2) using distilled water, 0.1 M HCl, 0.1 M HNO_3 and 0.1 M Na_2CO_3 . The results indicated that HNO_3 and Na_2CO_3 could effectively release U(VI) from 1-H, 1-OH, and 1- NH_2 with the desorption rate $\sim 80\%$. Especially, excessive amounts of anions (e.g., NO_3^- , SO_4^{2-} and Br^-) have been suggested as the superior triggers to competitively exchange the adsorbed metal species from MOFs (Fu et al., 2015; Li et al., 2015, 2017; Lv et al., 2017; Sheng et al., 2017). Fu et al. (2015) reported that Cr(VI) could be mostly released from FIR-53 after exposure to 200-fold molar excess of NO_3^- for 26 h. Also, five continuous trapping-releasing cycles could be achieved with 87% desorption rate of Cr(VI). Comparatively, no obvious desorption of Cr(VI) from FIR-54 was noted in the presence of the same amount of NO_3^- , whereas 91% regeneration rate was found when ClO_4^- was used as the ion-exchange trigger. Overall, these water-stable MOFs were reversibly regenerated using the proper eluents for successive adsorption of heavy metals and radionuclides.

9. Conclusions and outlook

Water-stable MOFs and MOF-based composites are green materials that exhibited the superior adsorption ability for removing target metal species. The adsorptive processes were generally fitted well with pseudo-second-order kinetic and Langmuir isotherm models. Several dominated adsorptive mechanisms were proposed, including the strong coordination between heavy metals/radionuclides and the binding sites (e.g., hydroxyl, thiol, amide substituents and other oxygen-containing groups) of organic ligands of water-stable MOFs, electrostatic interactions, anion exchange or SC-SC transformation, and combined adsorption-reduction process. Additionally, these materials also showed the excellent visible light-driven photocatalytic performance for reducing Cr(VI) by forming reactive photo-generating electrons in the systems and by decreasing the recombination of electron-hole pairs. Also, MOFs could catalyze the reduction of Cr(VI) by formic acid effectively, which appears to be a green technology in sustainable water purification. The superior selectivity, good stability, and reusability of MOFs during the treatments, indicating the promising applications of these emerging techniques for treating water and wastewater contaminated with different kinds of heavy metal ions and radionuclides.

There are still great challenges before applying MOFs in practical water treatment. The primary consideration is the upscale potential of synthesis, which has not been addressed adequately in literature. Nowadays, most of the MOFs are synthesized by solvothermal methods in organic solvents such as N,N'-dimethylformamide (DMF) and methanol. The impact of used solvent to the environment should be considered thoroughly. Negative effects of organics may be minimized by recycling the solvents. A progress is being in developing environmentally benign synthetic conditions of aqueous phase (Li et al., 2018) and solvent-free synthesis (Zou et al., 2016).

Additionally, electrochemical, microwave, and mechanical methods may have advantages when scaling up synthesis of MOFs is carried out.

The pore size of most of the reported MOFs is limited to micropore range, which might hamper the mobility of large metal ions inside the framework. Therefore, in future studies, researchers may modify structures of MOFs to fully utilize the abundant adsorption/conversion sites distributing throughout the fine structure. Generally, it would be beneficial to improve the adsorption kinetics by enlarging the pore size (Howarth et al., 2015, Yuan et al., 2017b, Feng et al., 2018) or reducing the size of MOF crystals (Wang et al., 2018).

In terms of aqueous removal and pollution elimination of heavy metals and radionuclides by the water-stable MOFs and MOF-based materials, future studies must improve their application potentials. This aim can be achieved by: (1) developing greener MOFs with ultrahigh porosity and enriched active sites through post-synthetic modifications (e.g., the introduction of multiple metal/organic functional groups or further complexity to the crystalline structures); (2) preparing novel and multifunctional MOF-based platforms such as hybrid MOF-on-MOF heteroarchitectures, defect-tunable MOFs and/or non-crystalline MOFs with liquid or amorphous (glass) phases; (3) synthesizing multi-component MOFs by chemical decorations with hybrid functional composites such as quantum dots, semiconductors, ionic liquids and carbon-based materials. Considering the mixed pollution by a wide range of hazardous heavy metal ions, radionuclides and organic contaminants (e.g., pharmaceutical residues and endocrine-disrupting chemicals) in real waters, it is desirable to investigate the performance and the mechanisms of innovative MOF materials for sustainable water purification. Additionally, further efforts may be directed towards improving the water stability of MOFs during successive practical applications. Also, development of robust and cost-effective MOFs with high selectivity and superior reusability

is also needed for depolluting toxic heavy metals and radionuclides in matrices such as soil, sediments and atmospheric particles. The application of water-stable MOFs to nuclear waste disposal may be elucidated in future studies.

Acknowledgment. Authors wish to thank anonymous reviewers for their comments, which improve the paper greatly.

References

- Abbasi, A., Moradpour, T., Van Hecke, K., 2015. A new 3D cobalt(II) metal-organic framework nanostructure for heavy metal adsorption. *Inorg. Chim. Acta* 430, 261-267.
- Abney, C.W., Gilhula, J.C., Lu, K., Lin, W., 2014a. Metal-organic framework templated inorganic sorbents for rapid and efficient extraction of heavy metals. *Adv. Mater.* 26, 7993-7996.
- Abney, C.W., Taylor-Pashow, K.M.L., Russell, S.R., Chen, Y., Samantaray, R., Lockard, J.V., Lin, W., 2014b. Topotactic transformations of metal-organic frameworks to highly porous and stable inorganic sorbents for efficient radionuclide sequestration. *Chem. Mater.* 26, 5231-5243.
- Abokifa, A.A., Biswas, P., 2017. Modeling soluble and particulate lead release into drinking water from full and partially replaced lead service lines. *Environ. Sci. Technol.* 51, 3318-3326.
- Aboutorabi, L., Morsali, A., Tahmasebi, E., Büyükgüngör, O., 2016. Metal-organic framework based on isonicotinate N-oxide for fast and highly efficient aqueous phase Cr(VI) adsorption. *Inorg. Chem.* 55, 5507-5513.
- Aguila, B., Banerjee, D., Nie, Z., Shin, Y., Ma, S., Thallapally, P.K., 2016. Selective removal of cesium and strontium using porous frameworks from high level nuclear waste. *Chem. Commun.* 52, 5940-5942.
- Ahmed, I., Jung, S.H., 2017. Applications of metal-organic frameworks in adsorption/separation processes via hydrogen bonding interactions. *Chem. Eng. J.* 310, 197-215.
- Akiya, N., Savage, P.E., 1998. Role of water in formic acid decomposition. *AIChE J.* 44, 405-415.

- Alqadami, A.A., Khan, M.A., Siddiqui, M.R., Alothman, Z.A., 2018. Development of citric anhydride anchored mesoporous MOF through post synthesis modification to sequester potentially toxic lead(II) from water. *Microporous Mesoporous Mater.* 261, 198-206.
- Audu, C.O., Nguyen, H.G.T., Chang, C., Katz, M.J., Mao, L., Farha, O.K., Hupp, J.T., Nguyen, S.T., 2016. The dual capture of As^V and As^{III} by UiO-66 and analogues. *Chem. Sci.* 7, 6492-6498.
- Babazadeh, M., Hosseinzadeh-Khanmiri, R., Abolhasani, J., Ghorbani-Kalhor, E., Hassanpour, A., 2015. Solid phase extraction of heavy metal ions from agricultural samples with the aid of a novel functionalized magnetic metal-organic framework. *RSC Adv.* 5, 19884-19892.
- Bai, J., Yin, X., Zhu, Y., Fan, F., Wu, X., Tian, W., Tan, C., Zhang, X., Wang, Y., Cao, S., Fan, F., Qin, Z., Guo, J., 2016. Selective uranium sorption from salt lake brines by amidoximated *Saccharomyces cerevisiae*. *Chem. Eng. J.* 283, 889-895.
- Bai, Z., Yuan, L., Zhu, L., Liu, Z., Chu, S., Zheng, L., Zhang, J., Chai, Z., Shi, W., 2015. Introduction of amino groups into acid-resistant MOFs for enhanced U(VI) sorption. *J. Mater. Chem. A* 3, 525-534.
- Banerjee, D., Xu, W., Nie, Z., Johnson, L.E.V., Coghlan, C., Sushko, M.L., Kim, D., Schweiger, M.J., Kruger, A.A., Doonan, C.J., Thallapally, P.K., 2016. Zirconium-based metal-organic framework for removal of perchlorate from water. *Inorg. Chem.* 55, 8241-8243.
- Bhattacharjee, S., Lee, Y., Ahn, W., 2015. Post-synthesis functionalization of a zeolitic imidazolate structure ZIF-90: A study on removal of Hg(II) from water and epoxidation of alkenes. *Crystengcomm.* 17, 2575-2582.
- Bosch, M., Yuan, S., Rutledge, W., Zhou, H.C., 2017. Stepwise synthesis of metal-organic frameworks. *Acc. Chem. Res.* 50, 857-865.
- Burtch, N.C., Jasuja, H., Walton, K.S., 2014. Water stability and adsorption in metal-organic frameworks. *Chem. Rev.* 114, 10575-10612.
- Cai, J., Wang, X., Zhou, Y., Jiang, L., Wang, C., 2016. Selective adsorption of arsenate and the reversible structure transformation of the mesoporous metal-organic framework MIL-100(Fe). *Phys. Chem. Chem. Phys.* 18, 10864-10867.
- Canivet, J., Fateeva, A., Guo, Y., Coasne, B., Farrusseng, D., 2014. Water adsorption in MOFs: Fundamentals and applications. *Chem. Soc. Rev.* 43, 5594-5617.
- Canlas, C.P., Lu, J., Ray, N.A., Grosso-Giordano, N.A., Lee, S., Elam, J.W., Winans, R.E., Van Duyne, R.P., Stair, P.C., Notestein, J.M., 2012. Shape-selective sieving layers on an oxide catalytic surface. *Nat. Chem.* 4, 1030-1036.

- Cao, C., Tan, C., Sindoro, M., Zhang, H., 2017. Hybrid micro-/nano-structures derived from metal-organic frameworks: preparation and applications in energy storage and conversion. *Chem. Soc. Rev.* 45, 2660-2677.
- Carboni, M., Abney, C.W., Liu, S., Lin, W., 2013. Highly porous and stable metal-organic frameworks for uranium extraction. *Chem. Sci.* 4, 2396-2402.
- Chang, Z., Yang, D., Xu, J., Hu, T., Bu, X., 2015. Flexible metal-organic frameworks: Recent advances and potential applications. *Adv. Mater.* 27, 5432-5441.
- Chen, J., Shen, K., Li, Y., 2017. Greening the processes of metal-organic framework synthesis and their use in sustainable catalysis. *ChemSusChem* 10, 3165-3187.
- Chen, L., Rangan, S., Li, J., Jiang, H., Li, Y., 2014. A molecular Pd(II) complex incorporated into a MOF as a highly active single-site heterogeneous catalyst for C-Cl bond activation. *Green Chem.* 16, 3978-3985.
- Cheng, M., Lai, C., Liu, Y., Zeng, G.M., Huang, D.L., Zhang, C., Qin, L., Hu, L., Zhou, C.Y., Xiong, W.P., 2018. Metal-organic frameworks for highly efficient heterogeneous Fenton-like catalysis. *Coordination Chemistry Reviews* 368, 80-92.
- Custelcean, R., Bonnesen, P.V., Duncan, N.C., Zhang, X., Watson, L.A., Van Berkel, G., Parson, W.B., Hay, B.P., 2012. Urea-functionalized M_4L_6 cage receptors: Anion-templated self-assembly and selective guest exchange in aqueous solutions. *J. Am. Chem. Soc.* 134, 8525-8534.
- De Decker, J., Folens, K., De Clercq, J., Meledina, M., Van Tendeloo, G., Du Laing, G., Van Der Voort, P., 2017. Ship-in-a-bottle CMPO in MIL-101(Cr) for selective uranium recovery from aqueous streams through adsorption. *J. Hazard. Mater.* 335, 1-9.
- Decoste, J.B., Peterson, G.W., 2014. Metal-organic frameworks for air purification of toxic chemicals. *Chem. Rev.* 114, 5695-5727.
- Delile, H., Keenan-Jones, D., Blichert-Toft, J., Goiran, J., Arnaud-Godet, F., Romano, P., Albarède, F., 2016. A lead isotope perspective on urban development in ancient Naples. *Proc. Natl. Acad. Sci. U. S. A.* 113, 6148-6153.
- Desai, A.V., Manna, B., Karmakar, A., Sahu, A., Ghosh, S.K., 2016. A water-stable cationic metal-organic framework as a dual adsorbent of oxoanion pollutants. *Angew. Chem. Int. Ed.* 55, 7811-7815.
- Deshommes, E., Bannier, A., Laroche, L., Nour, S., Prévost, M., 2016. Monitoring-based framework to detect and manage lead water service lines. *J. Am. Water Works Assoc.* 108, E555-E570.

- Dhakshinamoorthy, A., Asiri, A.M., Alvaro, M., Garcia, H., 2018. Metal organic frameworks as catalysts in solvent-free or ionic liquid assisted conditions. *Green Chem.* 20, 86-107.
- Dhakshinamoorthy, A., Asiri, A.M., Garcia, H., 2017. Metal organic frameworks as versatile hosts of Au nanoparticles in heterogeneous catalysis. *ACS Catal.* 7, 2896-2919.
- Dhakshinamoorthy, A., Asiri, A.M., García, H., 2016. Metal-organic framework (MOF) compounds: Photocatalysts for redox reactions and solar fuel production. *Angew. Chem. Int. Ed.* 55, 5414-5445.
- Ding, S., Yang, Y., Li, C., Huang, H., Hou, L., 2016. The effects of organic fouling on the removal of radionuclides by reverse osmosis membranes. *Water Res.* 95, 174-184.
- Elzwayie, A., Afan, H.A., Allawi, M.F., El-Shafie, A., 2017. Heavy metal monitoring, analysis and prediction in lakes and rivers: state of the art. *Environ. Sci. Pollut. Res.* 24, 12104-12117.
- Falcaro, P., Ricco, R., Yazdi, A., Imaz, I., Furukawa, S., Maspocho, D., Ameloot, R., Evans, J.D., Doonan, C.J., 2016. Application of metal and metal oxide nanoparticles at MOFs. *Coord. Chem. Rev.* 307, 237-254.
- Fang, Q., Yuan, D., Sculley, J., Li, J., Han, Z., Zhou, H.C., 2010. Functional mesoporous metal-organic frameworks for the capture of heavy metal ions and size-selective catalysis. *Inorg. Chem.* 49, 11637-11642.
- Fei, H., Bresler, M.R., Oliver, S.R.J., 2011. A new paradigm for anion trapping in high capacity and selectivity: Crystal-to-crystal transformation of cationic materials. *J. Am. Chem. Soc.* 133, 11110-11113.
- Fei, H., Han, C.S., Robins, J.C., Oliver, S.R.J., 2013. A cationic metal-organic solid solution based on Co(II) and Zn(II) for chromate trapping. *Chem. Mater.* 25, 647-652.
- Feng, D., Liu, T., Su, J., Bosch, M., Wei, Z., Wan, W., Yuan, D., Chen, Y., Wang, X., Wang, K., Lian, X., Gu, Z., Park, J., Zou, X., Zhou, H.C., 2015a. Stable metal-organic frameworks containing single-molecule traps for enzyme encapsulation. *Nat. Commun.* 6, 5979.
- Feng, D., Wang, K., Su, J., Liu, T., Park, J., Wei, Z., Bosch, M., Yakovenko, A., Zou, X., Zhou, H.C., 2015b. A highly stable zeotype mesoporous zirconium metal-organic framework with ultralarge pores. *Angew. Chem. Int. Ed.* 54, 149-154.
- Feng, D., Wang, K., Wei, Z., Chen, Y., Simon, C.M., Arvapally, R.K., Martin, R.L., Bosch, M., Liu, T., Fordham, S., Yuan, D., Omary, M.A., Haranczyk, M., Smit, B., Zhou, H.C., 2014. Kinetically tuned dimensional augmentation as a versatile synthetic route towards robust metal-organic frameworks. *Nat. Commun.* 5, 5723.

- Feng, L., Yuan, S., Zhang, L.L., Tan, K., Li, J.L., Kirchon, A., Liu, L.M., Zhang, P., Han, Y., Chabal, Y.J., Zhou, H.C., 2018. Creating hierarchical pores by controlled linker thermolysis in multivariate metal-organic frameworks. *J. Am. Chem. Soc.* 140, 2363-2372.
- Feng, M., Sarma, D., Qi, X., Du, K., Huang, X., Kanatzidis, M.G., 2016. Efficient removal and recovery of uranium by a layered organic-inorganic hybrid thiostannate. *J. Am. Chem. Soc.* 138, 12578-12585.
- Férey, C., Mellot-Draznieks, C., Serre, C., Millange, F., Dutour, J., Surblé, S., Margiolaki, I., 2005. Chemistry: A chromium terephthalate-based solid with unusually large pore volumes and surface area. *Science* 309, 2040-2042.
- Férey, G., Serre, C., Mellot-Draznieks, C., Millange, F., Surblé, S., Dutour, J., Margiolaki, I., 2004. A hybrid solid with giant pores prepared by a combination of targeted chemistry, simulation, and powder diffraction. *Angew. Chem. Int. Ed.* 43, 6296-6301.
- Folens, K., Leus, K., Nicomel, N.R., Meledina, M., Turner, S., Van Tendeloo, G., Laing, G.D., Van Der Voort, P., 2016. Fe₃O₄@MIL-101 – A selective and regenerable adsorbent for the removal of As species from water. *Eur. J. Inorg. Chem.* 2016, 4395-4401.
- Fu, F., Wang, Q., 2011. Removal of heavy metal ions from wastewaters: A review. *J. Environ. Manage.* 92, 407-418.
- Fu, H., Xu, Z., Zhang, J., 2015. Water-stable metal-organic frameworks for fast and high dichromate trapping via single-crystal-to-single-crystal ion exchange. *Chem. Mater.* 27, 205-210.
- Fu, Z., Guo, W., Dang, Z., Hu, Q., Wu, F., Feng, C., Zhao, X., Meng, W., Xing, B., Giesy, J.P., 2017. Refocusing on nonpriority toxic metals in the aquatic environment in China. *Environ. Sci. Technol.* 51, 3117-3118.
- Furukawa, H., Cordova, K.E., O'Keeffe, M., Yaghi, O.M., 2013. The chemistry and applications of metal-organic frameworks. *Science* 341, 1230444.
- Ghorbani-Kalhor, E., 2016. A metal-organic framework nanocomposite made from functionalized magnetite nanoparticles and HKUST-1 (MOF-199) for preconcentration of Cd(II), Pb(II), and Ni(II). *Microchim. Acta* 183, 2639-2647.
- Ghorbani-Kalhor, E., Hosseinzadeh-Khanmiri, R., Abolhasani, J., Babazadeh, M., Hassanpour, A., 2015. Determination of mercury(II) ions in seafood samples after extraction and preconcentration by a novel functionalized magnetic metal-organic framework nanocomposite. *J. Sep. Sci.* 38, 1179-1186.
- Ghorbani-Kalhor, E., Hosseinzadeh-Khanmiri, R., Babazadeh, M., Abolhasani, J., Hassanpour, A., 2014. Synthesis and application of a novel magnetic metal-organic framework

- nanocomposite for determination of Cd, Pb, and Zn in baby food samples. *Can. J. Chem.* 93, 518-525.
- Halder, S., Mondal, J., Ortega-Castro, J., Frontera, A., Roy, P., 2017. A Ni-based MOF for selective detection and removal of Hg^{2+} in aqueous medium: a facile strategy. *Dalton Trans.* 46, 1943-1950.
- Han, Y., Zheng, H., Liu, K., Wang, H., Huang, H., Xie, L., Wang, L., Li, J., 2016. In-situ ligand formation-driven preparation of a heterometallic metal-organic framework for highly selective separation of light hydrocarbons and efficient mercury adsorption. *ACS Appl. Mater. Inter.* 8, 23331-23337.
- Hasan, Z., Jhung, S.H., 2015. Removal of hazardous organics from water using metal-organic frameworks (MOFs): Plausible mechanisms for selective adsorptions. *J. Hazard. Mater.* 283, 329-339.
- Hassanpour, A., Hosseinzadeh-Khanmiri, R., Babazadeh, M., Abolhasani, J., Ghorbani-Kalhor, E., 2015. Determination of heavy metal ions in vegetable samples using a magnetic metal-organic framework nanocomposite sorbent. *Food Addit. Contam. A* 32, 725-736.
- He, Y., Tang, Y.P., Ma, D., Chung, T., 2017. UiO-66 incorporated thin-film nanocomposite membranes for efficient selenium and arsenic removal. *J. Membr. Sci.* 541, 262-270.
- Howarth, A.J., Katz, M.J., Wang, T.C., Platero-Prats, A.E., Chapman, K.W., Hupp, J.T., Farha, O.K., 2015. High efficiency adsorption and removal of selenate and selenite from water using metal-organic frameworks. *J. Am. Chem. Soc.* 137, 7488-7494.
- Hu, Y., Zhang, T., Li, M., Wang, Y., Zheng, Z., Zheng, Y., 2017. Copper(I)/(II)-redox triggered efficient and green rare-earth separation using a heterometallic metal-organic framework. *Green Chem.* 19, 1250-1254.
- Hua, M., Zhang, S., Pan, B., Zhang, W., Lv, L., Zhang, Q., 2012. Heavy metal removal from water/wastewater by nanosized metal oxides: A review. *J. Hazard. Mater.* 211-212, 317-331.
- Huang, L., He, M., Chen, B., Hu, B., 2016. A mercapto functionalized magnetic Zr-MOF by solvent-assisted ligand exchange for Hg^{2+} removal from water. *J. Mater. Chem. A* 4, 5159-5166.
- Huang, S., Gu, L., Zhu, N., Feng, K., Yuan, H., Lou, Z., Li, Y., Shan, A., 2014. Heavy metal recovery from electroplating wastewater by synthesis of mixed- $\text{Fe}_3\text{O}_4@/\text{SiO}_2$ /metal oxide magnetite photocatalysts. *Green Chem.* 16, 2696-2705.
- Huang, W., Liu, N., Zhang, X., Wu, M., Tang, L., 2017. Metal organic framework g- C_3N_4 /MIL-53(Fe) heterojunctions with enhanced photocatalytic activity for Cr(VI) reduction under visible light. *Appl. Surf. Sci.* 425, 107-116.

- Huang, Y., Zeng, X., Guo, L., Lan, J., Zhang, L., Cao, D., 2018. Heavy metal ion removal of wastewater by zeolite-imidazolate frameworks. *Sep. Purif. Technol.* 194, 462-469.
- Huo, J., Xu, L., Yang, J.E., Cui, H., Yuan, B., Fu, M., 2018. Magnetic responsive Fe₃O₄-ZIF-8 core-shell composites for efficient removal of As(III) from water. *Colloids Surf. A* 539, 59-68.
- Jamali, A., Tehrani, A.A., Shemirani, F., Morsali, A., 2016. Lanthanide metal-organic frameworks as selective microporous materials for adsorption of heavy metal ions. *Dalton Trans.* 45, 9193-9200.
- Jian, M., Liu, B., Zhang, G., Liu, R., Zhang, X., 2015. Adsorptive removal of arsenic from aqueous solution by zeolitic imidazolate framework-8 (ZIF-8) nanoparticles. *Colloids Surf. A* 465, 67-76.
- Jian, M., Wang, H., Liu, R., Qu, J., Wang, H., Zhang, X., 2016. Self-assembled one-dimensional MnO₂@zeolitic imidazolate framework-8 nanostructures for highly efficient arsenite removal. *Environ. Sci. Nano.* 3, 1186-1194.
- Julien, P.A., Mottillo, C., Frišćic, T., 2017. Metal-organic frameworks meet scalable and sustainable synthesis. *Green Chem.* 19, 2729-2747.
- Khan, N.A., Hasan, Z., Jung, S.H., 2013. Adsorptive removal of hazardous materials using metal-organic frameworks (MOFs): A review. *J. Hazard. Mater.* 244-245, 444-456.
- Khan, N.A., Jung, S.H., 2017. Adsorptive removal and separation of chemicals with metal-organic frameworks: Contribution of p-complexation. *J. Hazard. Mater.* 325, 198-213.
- Kim, J., Tsouris, C., Mayes, R.T., Oyola, Y., Saito, T., Janke, C.J., Dai, S., Schneider, E., Sachde, D., 2013. Recovery of uranium from seawater: A review of current status and future research needs. *Sep. Sci. Technol.* 48, 367-387.
- Kobielska, P.A., Howarth, A.J., Farha, O.K., Nayak, S., 2018. Metal-organic frameworks for heavy metal removal from water. *Coordin. Chem. Rev.* 358, 92-107.
- Laidlaw, M.A.S., Filippelli, G.M., Sadler, R.C., Gonzales, C.R., Ball, A.S., Mielke, H.W., 2016. Children's blood lead seasonality in flint, Michigan (USA), and soil-sourced lead hazard risks. *Int. J. Environ. Res. Public Health.* 13, 358.
- Lashley, M.A., Ivanov, A.S., Bryantsev, V.S., Dai, S., Hancock, R.D., 2016. Highly preorganized ligand 1,10-phenanthroline-2,9-dicarboxylic acid for the selective recovery of uranium from seawater in the presence of competing vanadium species. *Inorg. Chem.* 55, 10818-10829.
- Li, J., Liu, Y., Wang, X., Zhao, G., Ai, Y., Han, B., Wen, T., Hayat, T., Alsaedi, A., Wang, X., 2017. Experimental and theoretical study on selenate uptake to zirconium metal-organic frameworks: Effect of defects and ligands. *Chem. Eng. J.* 330, 1012-1021.

- Li, J., Wu, Y., Li, Z., Zhang, B., Zhu, M., Hu, X., Zhang, Y., Li, F., 2014a. Zeolitic imidazolate framework-8 with high efficiency in trace arsenate adsorption and removal from water. *J. Phys. Chem. C* 118, 27382-27387.
- Li, J., Wu, Y., Li, Z., Zhu, M., Li, F., 2014b. Characteristics of arsenate removal from water by metal-organic frameworks (MOFs). *Water Sci. Technol.* 70, 1391-1397.
- Li, J.Q., Gong, L.L., Feng, X.F., Zhang, L., Wu, H.Q., Yan, C.S., Xiong, Y.Y., Gao, H.Y., Luo, F., 2017. Direct extraction of U(VI) from alkaline solution and seawater via anion exchange by metal-organic framework. *Chem. Eng. J.* 316, 154-159.
- Li, J.R., Kuppler, R.J., Zhou, H.C., 2009. Selective gas adsorption and separation in metal-organic frameworks. *Chem. Soc. Rev.* 38, 1477-1504.
- Li, K., Lin, S.L., Li, Y.S., Zhuang, Q.X., Gu, J.L., 2018. Aqueous-phase synthesis of mesoporous Zr-based MOFs templated by amphoteric surfactants. *Angew. Chem. Int. Ed.* 57, 3439-3443.
- Li, L., Ma, W., Shen, S., Huang, H., Bai, Y., Liu, H., 2016. A combined experimental and theoretical study on the extraction of uranium by amino-derived metal-organic frameworks through post-synthetic strategy. *ACS Appl. Mater. Interfaces.* 8, 31032-31041.
- Li, L., Feng, X., Han, R., Zang, S., Yang, G., 2017. Cr(VI) removal via anion exchange on a silver-triazolate MOF. *J. Hazard. Mater.* 321, 622-628.
- Li, X., Gao, X., Ai, L., Jiang, J., 2015. Mechanistic insight into the interaction and adsorption of Cr(VI) with zeolitic imidazolate framework-67 microcrystals from aqueous solution. *Chem. Eng. J.* 274, 238-246.
- Li, X., Xu, H., Kong, F., Wang, R., 2013. A cationic metal-organic framework consisting of nanoscale cages: Capture, separation, and luminescent probing of $\text{Cr}_2\text{O}_7^{2-}$ through a single-crystal to single-crystal process. *Angew. Chem. Int. Ed.* 52, 13769-13773.
- Li, Z., Huang, Z., Guo, W., Wang, L., Zheng, L., Chai, Z., Shi, W., 2017. Enhanced photocatalytic removal of uranium(VI) from aqueous solution by magnetic $\text{TiO}_2/\text{Fe}_3\text{O}_4$ and its graphene composite. *Environ. Sci. Technol.* 51, 5666-5674.
- Li, Z., Yang, J., Sui, K., Yin, N., 2015. Facile synthesis of metal-organic framework MOF-808 for arsenic removal. *Mater Lett.* 160, 412-414.
- Liang, R., Chen, R., Jing, F., Qin, N., Wu, L., 2015a. Multifunctional polyoxometalates encapsulated in MIL-100(Fe): Highly efficient photocatalysts for selective transformation under visible light. *Dalton Trans.* 44, 18227-18236.
- Liang, R., Jing, F., Shen, L., Qin, N., Wu, L., 2015b. M@MIL-100(Fe) (M = Au, Pd, Pt) nanocomposites fabricated by a facile photodeposition process: Efficient visible-light photocatalysts for redox reactions in water. *Nano Res.* 8, 3237-3249.

- Liang, R., Jing, F., Shen, L., Qin, N., Wu, L., 2015c. MIL-53(Fe) as a highly efficient bifunctional photocatalyst for the simultaneous reduction of Cr(VI) and oxidation of dyes. *J. Hazard. Mater.* 287, 364-372.
- Liang, R., Shen, L., Jing, F., Qin, N., Wu, L., 2015d. Preparation of MIL-53(Fe)-reduced graphene oxide nanocomposites by a simple self-assembly strategy for increasing interfacial contact: Efficient visible-light photocatalysts. *ACS Appl. Mater. Inter.* 7, 9507-9515.
- Liang, R., Shen, L., Jing, F., Wu, W., Qin, N., Lin, R., Wu, L., 2015e. NH₂-mediated indium metal-organic framework as a novel visible-light-driven photocatalyst for reduction of the aqueous Cr(VI). *Appl. Catal. B Environ.* 162, 245-251.
- Lin, Z., Lü, J., Hong, M., Cao, R., 2014. Metal-organic frameworks based on flexible ligands (FL-MOFs): Structures and applications. *Chem. Soc. Rev.* 43, 5867-5895.
- Little, M.P., Wakeford, R., Bouville, A., Simon, S.L., 2016. Measurement of Fukushima-related radioactive contamination in aquatic species. *Proc. Natl. Acad. Sci. U. S. A.* 113, 3720-3721.
- Liu, B., Jian, M., Liu, R., Yao, J., Zhang, X., 2015. Highly efficient removal of arsenic(III) from aqueous solution by zeolitic imidazolate frameworks with different morphology. *Colloids Surf. A* 481, 358-366.
- Liu, S., Luo, M., Li, J., Luo, F., Ke, L., Ma, J., 2016. Adsorption equilibrium and kinetics of uranium onto porous azo-metal-organic frameworks. *J. Radioanal. Nucl. Chem.* 310, 353-362.
- Liu, T., Che, J., Hu, Y., Dong, X., Liu, X., Che, C., 2014. Alkenyl/thiol-derived metal-organic frameworks (MOFs) by means of postsynthetic modification for effective mercury adsorption. *Chem. Eur. J.* 20, 14090-14095.
- Liu, W., Dai, X., Bai, Z., Wang, Y., Yang, Z., Zhang, L., Xu, L., Chen, L., Li, Y., Gui, D., Diwu, J., Wang, J., Zhou, R., Chai, Z., Wang, S., 2017a. Highly sensitive and selective uranium detection in natural water systems using a luminescent mesoporous metal-organic framework equipped with abundant Lewis basic sites: A combined batch, X-ray absorption spectroscopy, and first principles simulation investigation. *Environ. Sci. Technol.* 51, 3911-3921.
- Liu, X., Zhou, Y., Zhang, J., Tang, L., Luo, L., Zeng, G., 2017b. Iron containing metal-organic frameworks: Structure, synthesis, and applications in environmental remediation. *ACS Appl. Mater. Inter.* 9, 20255-20275.
- Luo, B., Yuan, L., Chai, Z., Shi, W., Tang, Q., 2016. U(VI) capture from aqueous solution by highly porous and stable MOFs: UiO-66 and its amine derivative. *J. Radioanal. Nucl. Chem.* 307, 269-276.
- Luo, F., Chen, J.L., Dang, L.L., Zhou, W.N., Lin, H.L., Li, J.Q., Liu, S.J., Luo, M.B., 2015. High-performance Hg²⁺ removal from ultra-low-concentration aqueous solution using both

- acylamide- and hydroxyl-functionalized metal-organic framework. *J. Mater. Chem. A* 3, 9616-9620.
- Luo, J., Xu, F., Hu, J., Lin, P., Tu, J., Wu, X., Hou, X., 2017. Preconcentration on metal organic framework UiO-66 for slurry sampling hydride generation-atomic fluorescence spectrometric determination of ultratrace arsenic. *Microchem. J.* 133, 441-447.
- Luo, X., Ding, L., Luo, J., 2015. Adsorptive removal of Pb(II) ions from aqueous samples with amino-functionalization of metal-organic frameworks MIL-101(Cr). *J. Chem. Eng. Data* 60, 1732-1743.
- Luo, X., Shen, T., Ding, L., Zhong, W., Luo, J., Luo, S., 2016. Novel thymine-functionalized MIL-101 prepared by post-synthesis and enhanced removal of Hg²⁺ from water. *J. Hazard. Mater.* 306, 313-322.
- Lupa, L., Maranescu, B., Visa, A., 2017. Equilibrium and kinetic studies of chromium ions adsorption on Co (II)-based phosphonate metal organic frameworks. *Sep. Sci. Technol.* 53, 1017-1026.
- Lv, X., Shi, L., Li, K., Li, B., Li, H., 2017. An unusual porous cationic metal-organic framework based on a tetranuclear hydroxyl-copper(II) cluster for fast and highly efficient dichromate trapping through a single-crystal to single-crystal process. *Chem. Commun.* 53, 1860-1863.
- Ma, L., Wang, Q., Islam, S.M., Liu, Y., Ma, S., Kanatzidis, M.G., 2016. Highly selective and efficient removal of heavy metals by layered double hydroxide intercalated with the MoS₄²⁻ ion. *J. Am. Chem. Soc.* 138, 2858-2866.
- Masters, S., Welter, G.J., Edwards, M., 2016. Seasonal variations in lead release to potable water. *Environ. Sci. Technol.* 50, 5269-5277.
- Mon, M., Lloret, F., Ferrando-Soria, J., Martí-Gastaldo, C., Armentano, D., Pardo, E., 2016. Selective and efficient removal of mercury from aqueous media with the highly flexible arms of a BioMOF. *Angew. Chem. Int. Ed.* 55, 11167-11172.
- Nalaparaju, A., Jiang, J., 2012. Ion exchange in metal-organic framework for water purification: Insight from molecular simulation. *J. Phys. Chem. C* 116, 6925-6931.
- Nasir, A.M., Md Nordin, N.A.H., Goh, P.S., Ismail, A.F., 2018. Application of two-dimensional leaf-shaped zeolitic imidazolate framework (2D ZIF-L) as arsenite adsorbent: Kinetic, isotherm and mechanism. *J. Mol. Liq.* 250, 269-277.
- Nasrollahpour, A., Moradi, S.E., 2017. Hexavalent chromium removal from water by ionic liquid modified metal-organic frameworks adsorbent. *Micropor. Mesopor. Mater.* 243, 47-55.

- Niknam Shahrak, M., Ghahramaninezhad, M., Eydifarash, M., 2017. Zeolitic imidazolate framework-8 for efficient adsorption and removal of Cr(VI) ions from aqueous solution. *Environ. Sci. Pollut. Res.* 24, 9624-9634.
- Niu, H., Zheng, Y., Wang, S., He, S., Cai, Y., 2017. Stable hierarchical microspheres of 1D Fe-gallic acid MOFs for fast and efficient Cr(VI) elimination by a combination of reduction, metal substitution and coprecipitation. *J. Mater. Chem. A* 5, 16600-16604.
- Ogden, M.D., Moon, E.M., Wilson, A., Pepper, S.E., 2017. Application of chelating weak base resin Dowex M4195 to the recovery of uranium from mixed sulfate/chloride media. *Chem. Eng. J.* 317, 80-89.
- Park, K.S., Ni, Z., Côté, A.P., Choi, J.Y., Huang, R., Uribe-Romo, F.J., Chae, H.K., O'Keeffe, M., Yaghi, O.M., 2006. Exceptional chemical and thermal stability of zeolitic imidazolate frameworks. *Proc. Natl. Acad. Sci. U. S. A.* 103, 10186-10191.
- Peng, Y., Huang, H., Zhang, Y., Kang, C., Chen, S., Song, L., Liu, D., Zhong, C., 2018. A versatile MOF-based trap for heavy metal ion capture and dispersion. *Nat. Commun.* 9, 187.
- Pieper, K.J., Tang, M., Edwards, M.A., 2017. Flint water crisis caused by interrupted corrosion control: Investigating "ground zero" home. *Environ. Sci. Technol.* 51, 2007-2014.
- Qin, J., Tan, P., Jiang, Y., Liu, X., He, Q., Sun, L., 2016. Functionalization of metal-organic frameworks with cuprous sites using vapor-induced selective reduction: Efficient adsorbents for deep desulfurization. *Green Chem.* 18, 3210-3215.
- Rapti, S., Pournara, A., Sarma, D., Papadas, I.T., Armatas, G.S., Hassan, Y.S., Alkordi, M.H., Kanatzidis, M.G., Manos, M.J., 2016a. Rapid, green and inexpensive synthesis of high quality UiO-66 amino-functionalized materials with exceptional capability for removal of hexavalent chromium from industrial waste. *Inorg. Chem. Front.* 3, 635-644.
- Rapti, S., Pournara, A., Sarma, D., Papadas, I.T., Armatas, G.S., Tsipis, A.C., Lazarides, T., Kanatzidis, M.G., Manos, M.J., 2016b. Selective capture of hexavalent chromium from an anion-exchange column of metal organic resin-alginate composite. *Chem. Sci.* 7, 2427-2436.
- Ren, X.Y., Zeng, G.M., Tang, L., Wang, J.J., Wan, J., Feng, H.P., Song, B., Huang, C., Tang, X., 2018a. Effect of exogenous carbonaceous materials on the bioavailability of organic pollutants and their ecological risks. *Soil Biol. Biochem.* 116, 70-81.
- Ren, X.Y., Zeng, G.M., Tang, L., Wang, J.J., Wan, J., Liu, Y.N., Yu, J.F., Yi, H., Ye, S.J., Deng, R., 2018b. Sorption, transport and biodegradation – An insight into bioavailability of persistent organic pollutants in soil. *Sci. Total. Environ.* 610-611, 1154-1163.

- Ren, X.Y., Zeng, G.M., Tang, L., Wang, J.J., Wan, J., Wang, J.J., Deng, Y.C., Liu, Y.N., Peng, B., 2018c. The potential impact on the biodegradation of organic pollutants from composting technology for soil remediation. *Waste Manage.* 72, 138-149.
- Riccò, R., Liang, W., Li, S., Gassensmith, J.J., Caruso, F., Doonan, C., Falcaro, P., 2018. Metal-organic frameworks for cell and virus biology: A perspective. *ACS Nano.* 12, 13-23.
- Ricco, R., Konstas, K., Styles, M.J., Richardson, J.J., Babarao, R., Suzuki, K., Scopece, P., Falcaro, P., 2015. Lead(II) uptake by aluminium based magnetic framework composites (MFCs) in water. *J. Mater. Chem. A* 3, 19822-19831.
- Roushani, M., Saedi, Z., Baghelani, Y.M., 2017. Removal of cadmium ions from aqueous solutions using TMU-16-NH₂ metal organic framework. *Environ. Nanotechnol. Monit. Manag.* 7, 89-96.
- Salarian, M., Ghanbarpour, A., Behbahani, M., Bagheri, S., Bagheri, A., 2014. A metal-organic framework sustained by a nanosized Ag₁₂ cuboctahedral node for solid-phase extraction of ultra traces of lead(II) ions. *Microchim. Acta* 181, 999-1007.
- Saleem, H., Rafique, U., Davies, R.P., 2016. Investigations on post-synthetically modified UiO-66-NH₂ for the adsorptive removal of heavy metal ions from aqueous solution. *Micropor. Mesopor. Mater.* 221, 238-244.
- Schwarzenbach, R.P., Egli, T., Hofstetter, T.B., von Gunten, U., Wehrli, B., 2010. Global water pollution and human health. *Ann. Rev. Environ. Resour.* 35, 109-136.
- Seo, P.W., Song, J.Y., Jhung, S.H., 2016. Adsorptive removal of hazardous organics from water with metal-organic frameworks. *Appl. Chem. Eng.* 27, 358-365.
- Serre, C., Millange, F., Thouvenot, C., Noguès, M., Marsolier, G., Louër, D., Férey, G., 2002. Very large breathing effect in the first nanoporous chromium(III)-based solids: MIL-53 or Cr^{III}(OH)•{O₂C-C₆H₄-CO₂}•{HO₂C-C₆H₄-CO₂H}_x•H₂O_y. *J. Am. Chem. Soc.* 124, 13519-13526.
- Shao, L., Wang, X., Ren, Y., Wang, S., Zhong, J., Chu, M., Tang, H., Luo, L., Xie, D., 2016. Facile fabrication of magnetic cucurbit[6]uril/graphene oxide composite and application for uranium removal. *Chem. Eng. J.* 286, 311-319.
- Shen, K., Zhang, L., Chen, X., Liu, L., Zhang, D., Han, Y., Chen, J., Long, J., Luque, R., Li, Y., Chen, B., 2018. Ordered macro-microporous metal-organic framework single crystals. *Sci.* 359, 206-210.
- Shen, L., Huang, L., Liang, S., Liang, R., Qin, N., Wu, L., 2014. Electrostatically derived self-assembly of NH₂-mediated zirconium MOFs with graphene for photocatalytic reduction of Cr(VI). *RSC Adv.* 4, 2546-2549.

- Shen, L., Liang, R., Luo, M., Jing, F., Wu, L., 2015. Electronic effects of ligand substitution on metal-organic framework photocatalysts: The case study of UiO-66. *Phys. Chem. Chem. Phys.* 17, 117-121.
- Shen, L., Liang, S., Wu, W., Liang, R., Wu, L., 2013a. Multifunctional NH₂-mediated zirconium metal-organic framework as an efficient visible-light-driven photocatalyst for selective oxidation of alcohols and reduction of aqueous Cr(VI). *Dalton Trans.* 42, 13649-13657.
- Shen, L., Wu, W., Liang, R., Lin, R., Wu, L., 2013b. Highly dispersed palladium nanoparticles anchored on UiO-66(NH₂) metal-organic framework as a reusable and dual functional visible-light-driven photocatalyst. *Nanoscale.* 5, 9374-9382.
- Sheng, D., Zhu, L., Xu, C., Xiao, C., Wang, Y., Wang, Y., Chen, L., Diwu, J., Chen, J., Chai, Z., Albrecht-Schmitt, T.E., Wang, S., 2017. Efficient and selective uptake of TcO₄⁻ by a cationic metal-organic framework material with open Ag⁺ sites. *Environ. Sci. Technol.* 51, 3471-3479.
- Shi, L., Wang, T., Zhang, H., Chang, K., Meng, X., Liu, H., Ye, J., 2015. An amine-functionalized iron(III) metal-organic framework as efficient visible-light photocatalyst for Cr(VI) reduction. *Adv. Sci.* 2, 1500006.
- Shi, P., Zhao, B., Xiong, G., Hou, Y., Cheng, P., 2012. Fast capture and separation of, and luminescent probe for, pollutant chromate using a multi-functional cationic heterometal-organic framework. *Chem. Commun.* 48, 8231-8233.
- Shi, Z., Xu, C., Guan, H., Li, L., Fan, L., Wang, Y., Liu, L., Meng, Q., Zhang, R., 2018. Magnetic metal organic frameworks (MOFs) composite for removal of lead and malachite green in wastewater. *Colloids Surf. A* 539, 382-390.
- Singh, R., Singh, S., Parihar, P., Singh, V.P., Prasad, S.M., 2015. Arsenic contamination, consequences and remediation techniques: A review. *Ecotoxicol. Environ. Saf.* 112, 247-270.
- Smith, A.H., Steinmaus, C.M., 2009. Health effects of arsenic and chromium in drinking water: Recent human findings. *Annu. Rev. Public Health.* 30, 107-122.
- Sohrabi, M.R., Matbouie, Z., Asgharinezhad, A.A., Dehghani, A., 2013. Solid phase extraction of Cd(II) and Pb(II) using a magnetic metal-organic framework, and their determination by FAAS. *Microchim. Acta* 180, 589-597.
- Song, L.L., Chen, C., Luo, F., Huang, S.Y., Wang, L.L., Zhang, N., 2016. Isorecticular MOFs functionalized in the pore wall by different organic groups for high-performance removal of uranyl ions. *J. Radioanal. Nucl. Chem.* 310, 317-327.
- Steinhauser, G., 2014. Fukushimas forgotten radionuclides: A review of the understudied radioactive emissions. *Environ. Sci. Technol.* 48, 4649-4663.

- Taghizadeh, M., Asgharinezhad, A.A., Pooladi, M., Barzin, M., Abbaszadeh, A., Tadjarodi, A., 2013. A novel magnetic metal organic framework nanocomposite for extraction and preconcentration of heavy metal ions, and its optimization via experimental design methodology. *Microchim. Acta* 180, 1073-1084.
- Tahmasebi, E., Masoomi, M.Y., Yamini, Y., Morsali, A., 2015. Application of mechanosynthesized azine-decorated zinc(II) metal-organic frameworks for highly efficient removal and extraction of some heavy-metal ions from aqueous samples: A comparative study. *Inorg. Chem.* 54, 425-433.
- Tokalioglu, S., Yavuz, E., Demir, S., Patat, S., 2017. Zirconium-based highly porous metal-organic framework (MOF-545) as an efficient adsorbent for vortex assisted-solid phase extraction of lead from cereal, beverage and water samples. *Food Chem.* 237, 707-715.
- Trivedi, M., Bhaskaran, Kumar, A., Singh, G., Kumar, A., Rath, N.P., 2016. Metal-organic framework MIL-101 supported bimetallic Pd-Cu nanocrystals as efficient catalysts for chromium reduction and conversion of carbon dioxide at room temperature. *New J. Chem.* 40, 3109-3118.
- Vellingiri, K., Kim, K., Pournara, A., Deep, A., 2018. Towards high-efficiency sorptive capture of radionuclides in solution and gas. *Prog. Mater. Sci.* 94, 1-67.
- Vilela, D., Parmar, J., Zeng, Y., Zhao, Y., Sánchez, S., 2016. Graphene-based microbots for toxic heavy metal removal and recovery from water. *Nano Lett.* 16, 2860-2866.
- Villaescusa, I., Bollinger, J., 2008. Arsenic in drinking water: Sources, occurrence and health effects (a review). *Rev. Environ. Sci. Biotechnol.* 7, 307-323.
- Vu, T.A., Le, G.H., Dao, C.D., Dang, L.Q., Nguyen, K.T., Nguyen, Q.K., Dang, P.T., Tran, H.T.K., Duong, Q.T., Nguyen, T.V., Lee, G.D., 2015. Arsenic removal from aqueous solutions by adsorption using novel MIL-53(Fe) as a highly efficient adsorbent. *RSC Adv.* 5, 5261-5268.
- Wang, B., Lv, X., Feng, D., Xie, L., Zhang, J., Li, M., Xie, Y., Li, J.R., Zhou, H.C., 2016a. Highly stable Zr(IV)-based metal-organic frameworks for the detection and removal of antibiotics and organic explosives in water. *J. Am. Chem. Soc.* 138, 6204-6216.
- Wang, C., Lee, M., Liu, X., Wang, B., Paul Chen, J., Li, K., 2016b. A metal-organic framework/ α -alumina composite with a novel geometry for enhanced adsorptive separation. *Chem. Commun.* 52, 8869-8872.
- Wang, C., Liu, X., Chen, J.P., Li, K., 2015. Superior removal of arsenic from water with zirconium metal-organic framework UiO-66. *Sci. Rep.* 5, 16613.
- Wang, C., Liu, X., Keser Demir, N., Chen, J.P., Li, K., 2016a. Applications of water stable metal-organic frameworks. *Chem. Soc. Rev.* 45, 5107-5134.

- Wang, C., Du, X., Li, J., Guo, X., Wang, P., Zhang, J., 2016b. Photocatalytic Cr(VI) reduction in metal-organic frameworks: A mini-review. *Appl. Catal. B Environ.* 193, 198-216.
- Wang, C., Li, J., Lv, X., Zhang, Y., Guo, G., 2014. Photocatalytic organic pollutants degradation in metal-organic frameworks. *Energy Environ. Sci.* 7, 2831-2867.
- Wang, G., Zhang, H., Wang, J., Ling, Z., Qiu, J., 2017. In situ synthesis of chemically active ZIF coordinated with electrospun fibrous film for heavy metal removal with a high flux. *Sep. Purif. Technol.* 177, 257-262.
- Wang, H., Yuan, X., Wu, Y., Chen, X., Leng, L., Zeng, G., 2015a. Photodeposition of metal sulfides on titanium metal-organic frameworks for excellent visible-light-driven photocatalytic Cr(VI) reduction. *RSC Adv.* 5, 32531-32535.
- Wang, H., Yuan, X., Wu, Y., Zeng, G., Chen, X., Leng, L., Wu, Z., Jiang, L., Li, H., 2015b. Facile synthesis of amino-functionalized titanium metal-organic frameworks and their superior visible-light photocatalytic activity for Cr(VI) reduction. *J. Hazard. Mater.* 286, 187-194.
- Wang, K., Gu, J., Yin, N., 2017. Efficient removal of Pb(II) and Cd(II) using NH₂-functionalized Zr-MOFs via rapid microwave-promoted synthesis. *Ind. Eng. Chem. Res.* 56, 1880-1887.
- Wang, L.L., Luo, F., Dang, L.L., Li, J.Q., Wu, X.L., Liu, S.J., Luo, M.B., 2015. Ultrafast high-performance extraction of uranium from seawater without pretreatment using an acylamide- and carboxyl-functionalized metal-organic framework. *J. Mater. Chem. A* 3, 13724-13730.
- Wang, N., Ouyang, X., Yang, L., Omer, A.M., 2017. Fabrication of a magnetic cellulose nanocrystal/metal-organic framework composite for removal of Pb(II) from water. *ACS Sustain. Chem. Eng.* 5, 10447-10458.
- Wang, X.G., Cheng, Q., Yu, Y., Zhang, X.Z., 2018. Controlled nucleation and controlled growth for size predicable synthesis of nanoscale metal-organic frameworks (MOFs): A general and scalable approach. *Angew. Chem. Int. Ed.* 10.1002/anie.201803766.
- Wang, Y., Liu, Z., Li, Y., Bai, Z., Liu, W., Wang, Y., Xu, X., Xiao, C., Sheng, D., Diwu, J., Su, J., Chai, Z., Albrecht-Schmitt, T.E., Wang, S., 2015. Umbellate distortions of the uranyl coordination environment result in a stable and porous polycatenated framework that can effectively remove cesium from aqueous solutions. *J. Am. Chem. Soc.* 137, 6144-6147.
- Wang, Y., Xie, J., Wu, Y., Hu, X., 2014. A magnetic metal-organic framework as a new sorbent for solid-phase extraction of copper(II), and its determination by electrothermal AAS. *Microchim. Acta* 181, 949-956.
- Wen, J., Fang, Y., Zeng, G.M., 2018. Progress and prospect of adsorptive removal of heavy metal ions from aqueous solution using metal-organic frameworks: A review of studies from the last decade. *Chemosphere* 201, 627-643.

- Wu, S., Ge, Y., Wang, Y., Chen, X., Li, F., Xuan, H., Li, X., 2017. Adsorption of Cr(VI) on nano UiO-66-NH₂ MOFs in water. *Environ. Technol.* 1-12.
- Wu, X., Cobbina, S.J., Mao, G., Xu, H., Zhang, Z., Yang, L., 2016a. A review of toxicity and mechanisms of individual and mixtures of heavy metals in the environment. *Environ. Sci. Pollut. Res.* 23, 8244-8259.
- Wu, Y., Xu, G., Wei, F., Song, Q., Tang, T., Wang, X., Hu, Q., 2016b. Determination of Hg(II) in tea and mushroom samples based on metal-organic frameworks as solid phase extraction sorbents. *Micropor. Mesopor. Mater.* 235, 204-210.
- Wu, Y., Zhou, M., Zhang, B., Wu, B., Li, J., Qiao, J., Guan, X., Li, F., 2014. Amino acid assisted templating synthesis of hierarchical zeolitic imidazolate framework-8 for efficient arsenate removal. *Nanoscale* 6, 1105-1112.
- Xie, Z., Xu, W., Cui, X., Wang, Y., 2017. Recent progress in metal-organic frameworks and their derived nanostructures for energy and environmental applications. *ChemSusChem* 10, 1645-1663.
- Xiong, Y.Y., Li, J.Q., Yan, C.S., Gao, H.Y., Zhou, J.P., Gong, L.L., Luo, M.B., Zhang, L., Meng, P.P., Luo, F., 2016. MOF catalysis of Fe^{II}-to-Fe^{III} reaction for an ultrafast and one-step generation of the Fe₂O₃@MOF composite and uranium(VI) reduction by iron(II) under ambient conditions. *Chem. Commun.* 52, 9538-9541.
- Yadav, M., Xu, Q., 2013. Catalytic chromium reduction using formic acid and metal nanoparticles immobilized in a metal-organic framework. *Chem. Commun.* 49, 3327-3329.
- Yalfani, M.S., Contreras, S., Medina, F., Sueiras, J., 2008. Direct generation of hydrogen peroxide from formic acid and O₂ using heterogeneous Pd/ γ -Al₂O₃ catalysts. *Chem. Commun.* 3885-3887.
- Yang, J., Yin, X., 2017. CoFe₂O₄@MIL-100(Fe) hybrid magnetic nanoparticles exhibit fast and selective adsorption of arsenic with high adsorption capacity. *Sci. Rep.* 7, 40955.
- Yang, W., Bai, Z., Shi, W., Yuan, L., Tian, T., Chai, Z., Wang, H., Sun, Z., 2013. MOF-76: From a luminescent probe to highly efficient U^{VI} sorption material. *Chem. Commun.* 49, 10415-10417.
- Yee, K., Reimer, N., Liu, J., Cheng, S., Yiu, S., Weber, J., Stock, N., Xu, Z., 2013. Effective mercury sorption by thiol-laced metal-organic frameworks: In strong acid and the vapor phase. *J. Am. Chem. Soc.* 135, 7795-7798.
- Yin, N., Wang, K., Wang, L., Li, Z., 2016. Amino-functionalized MOFs combining ceramic membrane ultrafiltration for Pb(II) removal. *Chem. Eng. J.* 306, 619-628.

- Yin, N., Wang, K., Xia, Y., Li, Z., 2018. Novel melamine modified metal-organic frameworks for remarkably high removal of heavy metal Pb(II). *Desalination* 430, 120-127.
- Yu, C., Shao, Z., Hou, H., 2017. A functionalized metal-organic framework decorated with O-groups showing excellent performance for lead(II) removal from aqueous solution. *Chem. Sci.* 8, 7611-7619.
- Yu, S., Wang, X., Tan, X., Wang, X., 2015. Sorption of radionuclides from aqueous systems onto graphene oxide-based materials: A review. *Inorg. Chem. Front.* 2, 593-612.
- Yuan, G., Tian, Y., Liu, J., Tu, H., Liao, J., Yang, J., Yang, Y., Wang, D., Liu, N., 2017a. Schiff base anchored on metal-organic framework for Co(II) removal from aqueous solution. *Chem. Eng. J.* 326, 691-699.
- Yuan, S., Chen, Y., Qin, J., Lu, W., Zou, L., Zhang, Q., Wang, X., Sun, X., Zhou, H.C., 2016. Linker installation: Engineering pore environment with precisely placed functionalities in zirconium MOFs. *J. Am. Chem. Soc.* 138, 8912-8919.
- Yuan, S., Lu, W., Chen, Y., Zhang, Q., Liu, T., Feng, D., Wang, X., Qin, J., Zhou, H.C., 2015. Sequential linker installation: Precise placement of functional groups in multivariate metal-organic frameworks. *J. Am. Chem. Soc.* 137, 3177-3180.
- Yuan, S., Zou, L., Qin, J., Li, J., Huang, L., Feng, L., Wang, X., Bosch, M., Alsalme, A., Cagin, T., Zhou, H.C., 2017b. Construction of hierarchically porous metal-organic frameworks through linker labilization. *Nat. Commun.* 8, 15356.
- Zeng, T., Zhang, X., Wang, S., Niu, H., Cai, Y., 2015. Spatial confinement of a Co_3O_4 catalyst in hollow metal-organic frameworks as a nanoreactor for improved degradation of organic pollutants. *Environ. Sci. Technol.* 49, 2350-2357.
- Zhang, N., Yuan, L., Guo, W., Luo, S., Chai, Z., Shi, W., 2017. Extending the use of highly porous and functionalized MOFs to Th(IV) capture. *ACS Appl. Mater. Inter.* 9, 25216-25224.
- Zhang, Q., Yu, J., Cai, J., Zhang, L., Cui, Y., Yang, Y., Chen, B., Qian, G., 2015. A porous Zr-cluster-based cationic metal-organic framework for highly efficient $\text{Cr}_2\text{O}_7^{2-}$ removal from water. *Chem. Commun.* 51, 14732-14734.
- Zhang, T., Lin, W., 2014. Metal-organic frameworks for artificial photosynthesis and photocatalysis. *Chem. Soc. Rev.* 43, 5982-5993.
- Zhang, X., Shen, B., Zhu, S., Xu, H., Tian, L., 2016a. UiO-66 and its Br-modified derivatives for elemental mercury removal. *J. Hazard. Mater.* 320, 556-563.
- Zhang, X., Sarma, D., Wu, Y., Wang, L., Ning, Z., Zhang, F., Kanatzidis, M.G., 2016b. Open-framework oxysulfide based on the supertetrahedral $[\text{In}_4\text{Sn}_{16}\text{O}_{10}\text{S}_{34}]^{12-}$ cluster and efficient sequestration of heavy metals. *J. Am. Chem. Soc.* 138, 5543-5546.

- Zhang, Y., Yuan, S., Day, G., Wang, X., Yang, X., Zhou, H.C., 2018. Luminescent sensors based on metal-organic frameworks. *Coord. Chem. Rev.* 354, 28-45.
- Zhao, H., Xia, Q., Xing, H., Chen, D., Wang, H., 2017. Construction of pillared-layer MOF as efficient visible-light photocatalysts for aqueous Cr(VI) reduction and dye degradation. *ACS Sustain. Chem. Eng.* 5, 4449-4456.
- Zhao, M., Ou, S., Wu, C., 2014. Porous metal-organic frameworks for heterogeneous biomimetic catalysis. *Acc. Chem. Res.* 47, 1199-1207.
- Zhitkovich, A., 2011. Chromium in drinking water: Sources, metabolism, and cancer risks. *Chem. Res. Toxicol.* 24, 1617-1629.
- Zhou, H.C., Kitagawa, S., 2014. Metal-organic frameworks (MOFs). *Chem. Soc. Rev.* 43, 5415-5418.
- Zhu, B., Yu, X., Jia, Y., Peng, F., Sun, B., Zhang, M., Luo, T., Liu, J., Huang, X., 2012. Iron and 1,3,5-benzenetricarboxylic metal-organic coordination polymers prepared by solvothermal method and their application in efficient As(V) removal from aqueous solutions. *J. Phys. Chem. C* 116, 8601-8607.
- Zhu, K., Chen, C., Xu, H., Gao, Y., Tan, X., Alsaedi, A., Hayat, T., 2017a. Cr(VI) reduction and immobilization by core-double-shell structured magnetic polydopamine@zeolitic idazolate frameworks-8 microspheres. *ACS Sustain. Chem. Eng.* 5, 6795-6802.
- Zhu, L., Xiao, C., Dai, X., Li, J., Gui, D., Sheng, D., Chen, L., Zhou, R., Chai, Z., Albrecht-Schmitt, T.E., Shuao, W., 2017b. Exceptional perhenate/pertechnetate uptake and subsequent immobilization by a low-dimensional cationic coordination polymer: Overcoming the hofmeister bias selectivity. *Environ. Sci. Technol. Lett.* 4, 316-322.
- Zou, C., Vagin, S., Kronast, A., Rieger, B., 2016. Template mediated and solvent-free route to a variety of UiO-66 metal-organic frameworks. *RSC Adv.* 6, 102968.
- Zou, Y., Wang, X., Khan, A., Wang, P., Liu, Y., Alsaedi, A., Hayat, T., Wang, X., 2016a. Environmental remediation and application of nanoscale zero-valent iron and its composites for the removal of heavy metal ions: A review. *Environ. Sci. Technol.* 50, 7290-7304.
- Zou, Z., Wang, S., Jia, J., Xu, F., Long, Z., Hou, X., 2016b. Ultrasensitive determination of inorganic arsenic by hydride generation-atomic fluorescence spectrometry using Fe₃O₄@ZIF-8 nanoparticles for preconcentration. *Microchem. J.* 124, 578-583.

Table 1. Summary of adsorptive capability of MOFs and MOF-based composites for As species (As(III) and/or As(V)) in water.

Adsorbents (Ads.)	Reaction conditions	q_{\max} (mg/g)		Ref.
		As(III)	As(V)	
Fe-BTC	[As(V)] = 5 mg/L, [Ads.] = 5.0 g/L, pH 4, T = 298 K		12.29	(Zhu et al., 2012)
MIL-53(Al)	[As(V)] = 0.34 mg/L, [Ads.] = 20 mg/L, pH 8, T = 298 K		105.6	(Li et al., 2014b)
MIL-53(Fe)	[As(V)] = 5 mg/L, [Ads.] = 1.0 g/L, pH 5, T = 298 K		21.27	(Vu et al., 2015)
MIL-100(Fe)	[As(V)] = 10 mg/L, [Ads.] = 0.4 g/L, T = 298 K		110	(Cai et al., 2016)
MOF-808	[As(V)] = 5 mg/L, [Ads.] = 0.2 g/L, RT		24.83	(Li et al., 2015)
UiO-66	[As(V)] = 50 mg/L, [Ads.] = 0.5 g/L, pH 2, T = 298 K		303	(Wang et al., 2015)
ZIF-8	[As(V)] = 0-5 mg/L, [Ads.] = 40 mg/L, T = 298 K		76.5	(Li et al., 2014a)
ZIF-8	[As(III)/As(V)] = 20 mg/L, [Ads.] = 0.2 g/L, pH 7, T = 298 K	49.49	60.03	(Jian et al., 2015)
Cubic ZIF-8	[As(III)] = 0.2 mg/L, [Ads.] = 0.2 g/L, pH 8.5, T = 298 K	122.6		(Liu et al., 2015)
Dodecahedral ZIF-8	[As(III)] = 0.2 mg/L, [Ads.] = 0.2 g/L, pH 8.5, T = 298 K	117.5		(Liu et al., 2015)
Hierarchical ZIF-8	[As(V)] = 5 mg/L, [Ads.] = 40 mg/L, T = 298 K		90.92	(Wu et al., 2014)
Leaf-shaped ZIF-8	[As(III)] = 0.2 mg/L, [Ads.] = 0.2 g/L, pH 8.5, T = 298 K	108.1		(Liu et al., 2015)
2D-ZIF-L	[As(III)] = 10.0 mg/L, [Ads.] = 0.1 g/L, pH 10, T = 298 K	43.74		(Nasir et al., 2018)
β -MnO ₂ @ZIF-8	[As(III)] = 5-130 mg/L, [Ads.] = 0.2 g/L, pH 7, T = 298 K	140.27		(Jian et al., 2016)
CoFe ₂ O ₄ @MIL-100(Fe)	[As(III)/As(V)] = 1 mg/L, [Ads.] = 0.5 g/L, T = 298 K	143.6	114.8	(Yang and Yin, 2017)
Fe ₃ O ₄ @MIL-101(Cr)	[As(III)/As(V)] = 10 mg/L, [Ads.] = 3.84 g/L, pH 7, T = 298 K	121.5	80.0	(Folens et al., 2016)
Fe ₃ O ₄ @ZIF-8	[As(III)] = 3.5-40 mg/L, [Ads.] = 0.2 g/L, pH 8	100		(Huo et al., 2018)

Note: Fe-BTC, iron-1,3,5-benzenetricarboxylic polymer; RT, room temperature.

Table 2. Summary of adsorptive capability of MOFs and MOF-based composites for Pb(II), Hg(II), Cd(II), Cu(II), Ni(II), Zn(II), Co(II) and Mn(II) in water.

Adsorbents (Ads.)	Reaction conditions	q_{\max} (mg/g)	Ref.
Pb(II)	[Ag ₁₂ (MA) ₈ (mal) ₆ •18H ₂ O] _n	[Pb(II)] = 2 mg/L, [Ads.] = 4 g/L, pH 7	120 (Salarian et al., 2014)
	AMCA-MIL-53(Al)	[Pb(II)] = 25-400 mg/L, [Ads.] = 0.15 g/L, pH 5.8, T = 318 K	390 (Alqadami et al., 2018)
Dy-MOF	MCNC@Zn-BTC	[Pb(II)] = 1 mg/L, [Ads.] = 0.2 g/L, pH 6.5	3.05 (Jamali et al., 2016)
		[Pb(II)] = 200 mg/L, [Ads.] = 1 g/L, pH 2-6, T = 298.2 K	558.66 (Wang et al., 2017)
Melamine-MOFs		[Pb(II)] = 10 mg/L, [Ads.] = 0.04 g/L, pH 5, T = 313 K	122.0 (Yin et al., 2018)
MIL-101(Cr)		[Pb(II)] = 50 mg/L, [Ads.] = 1 g/L, pH 2.01, T = 298 K	15.78 (Luo et al., 2015)
ED-MIL-101(Cr) (5 mmol)		[Pb(II)] = 50 mg/L, [Ads.] = 1 g/L, pH 2.10, T = 298 K	81.09 (Luo et al., 2015)
MOF-545		[Pb(II)] = 0.2 mg/L, [Ads.] = 0.5 g/L, pH 7	73 (Tokalioglu et al., 2017)
MOF-808-EDTA		[Pb(II)] = 10 mg/L, [Ads.] = 1 g/L, RT	313 (Peng et al., 2018)
MOF-DHz		[Pb(II)] = 1 mg/L, [Ads.] = 5 g/L, pH 6.4	104 (Taghizadeh et al., 2013)
NH ₂ -Zr-MOFs		[Pb(II)] = 10 mg/L, [Ads.] = 0.04 g/L, pH 6, T = 303 K	166.74 (Wang et al., 2017)
TMU-4		[Pb(II)] = 0.1 mg/L, [Ads.] = 7 mg/30 mL, pH = 10	237 (Tahmasebi et al., 2015)
TMU-5		[Pb(II)] = 0.1 mg/L, [Ads.] = 7 mg/30 mL, pH = 10	251 (Tahmasebi et al., 2015)
TMU-6		[Pb(II)] = 0.1 mg/L, [Ads.] = 7 mg/30 mL, pH = 10	224 (Tahmasebi et al., 2015)
UiO-66-NHC(S)NHMe		[Pb(II)] = 100 mg/L, [Ads.] = 1 g/L	232 (Saleem et al., 2016)
ZIF-8		[Pb(II)] = 200 mg/L, [Ads.] = 0.1-2.0 g/L, pH 5.1, T = 298 K	1119.80 (Huang et al., 2018)
ZIF-67		[Pb(II)] = 200 mg/L, [Ads.] = 0.1-2.0 g/L, pH 5.2, T = 298 K	1348.42 (Huang et al., 2018)
[Zn ₃ L ₃ (BPE) _{1.5}] _n		[Pb(II)] = 10 mg/L, [Ads.] = 0.125 g/L, pH 6, T = 298 K	616.64 (Yu et al., 2017)
Fe ₃ O ₄ @Cu-MOFs		[Pb(II)] = 10-1000 mg/L, [Ads.] = 10 g/L	219.00 (Shi et al., 2018)
Fe ₃ O ₄ @TAR		[Pb(II)] = 1 mg/L, [Ads.] = 10 g/L, pH 6.2	185 (Ghorbani-Kalhor, 2016)
(Fe ₃ O ₄ -ED)/MIL-101(Fe)		[Pb(II)] = 0.5 mg/L, [Ads.] = 29 mg/7.0 mL, pH 6.1	198 (Babazadeh et al., 2015)
IOMN@NH ₂ -MIL53(Al)		[Pb(II)] = 100 mg/L, [Ads.] = 100 mg/15 mL	492.4 (Ricco et al., 2015)
Hg(II)	JUC-62	[Hg(II)] = 400 mg/L, [Ads.] = 1 g/L, RT	836.7 (Wu et al., 2016b)
	MFC-S	[Hg(II)] = 20 mg/L, [Ads.] = 1 g/L, RT	282 (Huang et al., 2016)
	MIL-101-NH ₂	[Hg(II)] = 20-220 mg/L, [Ads.] = 1 g/L, pH 6	30.67 (Luo et al., 2016)
	MIL-101-Thymine	[Hg(II)] = 20-220 mg/L, [Ads.] = 1 g/L, pH 6	51.75 (Luo et al., 2016)
	MOF-808-EDTA	[Hg(II)] = 10 mg/L, [Ads.] = 1 g/L, RT	592 (Peng et al., 2018)
	[Ni(3-bpd) ₂ (NCS) ₂] _n	Saturated Hg(II), [Ads.] = 1 g/L	713 (Halder et al., 2017)
	UiO-66-NHC(S)NHMe	[Hg(II)] = 100 mg/L, [Ads.] = 1 g/L	769 (Saleem et al., 2016)
	ZIF-90-SH	[Hg(II)] = 0.1-50 mg/L, [Ads.] = 1 g/L, T = 298 K	22.4 (Bhattacharjee et al., 2015)

	Zn(hip)(L)-(DMF)(H ₂ O)	[Hg(II)] = 0.1 mg/L, [Ads.] = 0.5 g/L, pH 5, T = 298 K	278	(Luo et al., 2015)
	Fe ₃ O ₄ @DMcT/MIL-101(Fe)	[Hg(II)] = 15 mg/L, $M_{\text{adsorbent}} = 28 \text{ mg/10 mL}$, pH 6.25	124	(Ghorbani-Kalhor et al., 2015)
Cd(II)	(Fe ₃ O ₄ -ED)/MIL-101(Fe)	[Cd(II)] = 0.5 mg/L, [Ads.] = 29 mg/7.0 mL, pH 6.1	155	(Babazadeh et al., 2015)
	Fe ₃ O ₄ @TAR	[Cd(II)] = 1 mg/L, [Ads.] = 10 g/L, pH 6.2	210	(Ghorbani-Kalhor, 2016)
	MOF-DHz	[Cd(II)] = 1 mg/L, [Ads.] = 5 g/L, pH 6.4	188	(Taghizadeh et al., 2013)
	NH ₂ -Zr-MOFs	[Cd(II)] = 10 mg/L, [Ads.] = 0.04 g/L, pH 6, T = 303 K	177.35	(Wang et al., 2017)
	TMU-16-NH ₂	[Cd(II)] = 50-200 mg/L, [Ads.] = 2 g/L, pH 6	126.6	(Roushani et al., 2017)
	TMU-4	[Cd(II)] = 0.1 mg/L, [Ads.] = 7 mg/30 mL, pH 10	48	(Tahmasebi et al., 2015)
	TMU-5	[Cd(II)] = 0.1 mg/L, [Ads.] = 7 mg/30 mL, pH 10	43	(Tahmasebi et al., 2015)
	TMU-6	[Cd(II)] = 0.1 mg/L, [Ads.] = 7 mg/30 mL, pH 10	41	(Tahmasebi et al., 2015)
	UiO-66-NHC(S)NHMe	[Cd(II)] = 100 mg/L, [Ads.] = 1 g/L	49	(Saleem et al., 2016)
Cu(II)	Dy-MOF	[Cu(II)] = 1 mg/L, [Ads.] = 0.2 g/L, pH 6.5	2.24	(Jamali et al., 2016)
	Fe ₃ O ₄ /IRMOF-3	[Cu(II)] = 1 mg/L, [Ads.] = 0.2 g/L, pH 5, RT	2.4	(Wang et al., 2014)
	TMU-4	[Cu(II)] = 0.1 mg/L, [Ads.] = 7 mg/30 mL, pH 10	62	(Tahmasebi et al., 2015)
	TMU-5	[Cu(II)] = 0.1 mg/L, [Ads.] = 7 mg/30 mL, pH 10	57	(Tahmasebi et al., 2015)
	TMU-6	[Cu(II)] = 0.1 mg/L, [Ads.] = 7 mg/30 mL, pH 10	60	(Tahmasebi et al., 2015)
	ZIF-8	[Cu(II)] = 200 mg/L, [Ads.] = 0.1-2.0 g/L, pH 5.1, T = 298 K	454.72	(Huang et al., 2018)
	ZIF-67	[Cu(II)] = 200 mg/L, [Ads.] = 0.1-2.0 g/L, pH 5.2, T = 298 K	617.51	(Huang et al., 2018)
Ni(II)	Fe ₃ O ₄ @TAR	[Ni(II)] = 1 mg/L, [Ads.] = 10 g/L, pH 6.2	196	(Ghorbani-Kalhor, 2016)
	MOF-DHz	[Ni(II)] = 1 mg/L, [Ads.] = 5 g/L, pH 6.4	98	(Taghizadeh et al., 2013)
Zn(II)	MOF-DHz	[Zn(II)] = 1 mg/L, [Ads.] = 5 g/L, pH 6.4	206	(Taghizadeh et al., 2013)
	(Fe ₃ O ₄ -ED)/MIL-101(Fe)	[Zn(II)] = 0.5 mg/L, [Ads.] = 29 mg/7.0 mL, pH 6.1	164	(Babazadeh et al., 2015)
Co(II)	TMU-4	[Co(II)] = 0.1 mg/L, [Ads.] = 7 mg/30 mL, pH 10	55	(Tahmasebi et al., 2015)
	TMU-5	[Co(II)] = 0.1 mg/L, [Ads.] = 7 mg/30 mL, pH 10	63	(Tahmasebi et al., 2015)
	TMU-6	[Co(II)] = 0.1 mg/L, [Ads.] = 7 mg/30 mL, pH 10	59	(Tahmasebi et al., 2015)
	UiO-66-Schiff	[Co(II)] = 0.1 mg/L, [Ads.] = 7 mg/30 mL, pH 10	256	(Yuan et al., 2017)
Mn(VII)	SLUG-21	[Mn(VII)] = 200 mg/L, [Ads.] = 0.5 g/L, RT	292	(Fei et al., 2011)

Note: DTIM, 4-(5)-imidazoledithiocarboxylic acid; H₂hip, 5-hydroxyisophthalic acid; IOMN, iron(II,III) oxide magnetic nanoparticles; L = *N*⁴,*N*^{4'}-di(pyridine-4-yl)biphenyl-4,4'-dicarboxamide; ED, ethylenediamine; TAR, 4-(thiazolylazo) resorcinol.

Table 3. Summary of adsorptive capability of MOFs and MOF-based composites for Cr species (Cr(III) or Cr(VI)) in water.

Adsorbents (Ads.)	Reaction conditions	q_{\max} (mg/g)		Ref.
		Cr(III)	Cr(VI)	
Ag-triazolate MOF	[Cr(VI)] = 50 mg/L, [Ads.] = 0.8 g/L, pH 6, T = 303 K		37	(Li et al., 2017)
{[Cu ₄ (μ ₃ -OH) ₂ (mtrb) ₂ (1,4-bda) ₂]Br ₂ ·6H ₂ O} _n	[Cr(VI)] = 2.5 mM, [Ads.] = 2.5 mM		128	(Lv et al., 2017)
Co-CP	[Cr(VI)] = 5-250 mg/L, [Ads.] = 2 g/L, pH 2.5		38.5	(Lupa et al., 2017)
Co-Gly	[Cr(VI)] = 5-250 mg/L, [Ads.] = 2 g/L, pH 2.5		43.5	(Lupa et al., 2017)
Co-VP	[Cr(VI)] = 5-250 mg/L, [Ads.] = 2 g/L, pH 2.5		49	(Lupa et al., 2017)
1D Fe-gallic acid	[Cr(VI)] = 100-2000 mg/L, [Ads.] = 1 g/L, pH 3-10, T = 298 K		1709.2	(Niu et al., 2017)
3D Dy-MOFs	[Cr(VI)] = 5 mM, [Ads.] = 7.8 g/L, RT		62.88	(Shi et al., 2012)
FIR-53	[Cr(VI)] = 2 mM, [Ads.] = 15 g/L, RT		74.2	(Fu et al., 2015)
FIR-54	[Cr(VI)] = 2 mM, [Ads.] = 15 g/L, RT		103	(Fu et al., 2015)
IL-MIL-100(Fe)	[Cr(VI)] = 100 mg/L, [Ads.] = 0.5 g/L, pH 2, T = 298-328 K		285.7	(Nasrollahpour and Moradi, 2017)
MOF-867	[Cr(VI)] = 50 mg/L, [Ads.] = 0.5 g/L, RT		53.4	(Zhang et al., 2015)
Protonated MOR-1	[Cr(VI)] = 21.6 mg/L, pH 3		247	(Rapti et al., 2016b)
Non-protonated MOR-1	[Cr(VI)] = 21.6 mg/L, pH 3		267	(Rapti et al., 2016b)
MOR-1-HA	[Cr(VI)] = 21.6 mg/L, pH 3		242	(Rapti et al., 2016b)
SLUG-21	[Cr(VI)] = 63.3 μM, [Ads.] = 0.5 g/L, RT		60	(Fei et al., 2011)
[[Ni ₂ (L) ₃ -(SO ₄)(H ₂ O) ₃]·(SO ₄)·x(G)] _n	[Cr(VI)] = 1 μM, [Ads.] = 1 g/L, RT		166	(Desai et al., 2016)
TMU-4	[Cr(III)] = 0.1 mg/L, [Ads.] = 7 mg/30 mL, pH 10	127		(Tahmasebi et al., 2015)
TMU-5	[Cr(III)] = 0.1 mg/L, [Ads.] = 7 mg/30 mL, pH 10	123		(Tahmasebi et al., 2015)
TMU-6	[Cr(III)] = 0.1 mg/L, [Ads.] = 7 mg/30 mL, pH 10	118		(Tahmasebi et al., 2015)
TMU-30	[Cr(VI)] = 30 mg/L, [Ads.] = 0.2 g/L		145	(Aboutorabi et al., 2016)
UiO-66-HA	[Cr(VI)] = 21.6 mg/L, pH 3		129	(Rapti et al., 2016b)
UiO-66-NH ₂	[Cr(VI)] = 5 mg/L, [Ads.] = 1 g/L, pH 6.5, T = 298 K		32.36	(Wu et al., 2017)
UiO-66-NHC(S)NHMe	[Cr(III)] = 100 mg/L, [Ads.] = 1 g/L	117		(Saleem et al., 2016)
ZIF-8	[Cr(VI)] = 2.5 mg/L, [Ads.] = 20 mg/L, pH 7, T = 298 K		0.15	(Niknam Shahrak et al., 2017)
ZIF-67	[Cr(VI)] = 6-15 mg/L, [Ads.] = 1 g/L, natural pH, RT		15.43	(Li et al., 2015)
ZJU-101	[Cr(VI)] = 50 mg/L, [Ads.] = 0.5 g/L, RT		245	(Zhang et al., 2015)
Zn _{0.5} Co _{0.5} -SLUG-35	[Cr(VI)] = 272 mg/L, [Ads.] = 2 g/L, pH 8.16, RT		68.5	(Fei et al., 2013)
MP@ZIF-8	[Cr(VI)] = 30 mg/L, [Ads.] = 0.2 g/L, pH 5, T = 293 K		136.56	(Zhu et al., 2017a)

Note: HA, alginate acid; MP, magnetic polydopamine; 1-SO₄, [[Ni₂(L)₃-(SO₄)(H₂O)₃]·(SO₄)·x(G)]_n (L = tris(4-(1H-imidazol-1-yl)phenyl)amine; G = DMF, H₂O).

Table 4. Summary of reductive transformation of Cr(VI) by MOFs and MOF-based composites in water.

Catalysts (Cat.)	Reaction conditions	Time (min)	Reductive rate (%)	Ref.
MIL-100(Fe)	[Cr(VI)] = 20 mg/L, [Cat.] = 1 g/L, pH 4, vis	24	100	(Liang et al., 2015b)
MIL-101(Fe)	[Cr(VI)] = 8 mg/L, [Cat.] = 0.5 g/L, pH 2, T = 303 K, vis	60	100	(Shi et al., 2015)
MIL-53(Fe)	[Cr(VI)] = 20 mg/L, [Cat.] = 1 g/L, pH 4, T = 303 K, vis	40	100	(Liang et al., 2015c)
MIL-68(In)-NH ₂	[Cr(VI)] = 20 mg/L, [Cat.] = 1 g/L, pH 6, T = 303 K, vis	180	97	(Liang et al., 2015e)
NH ₂ -MIL-125(Ti)	[Cr(VI)] = 48 mg/L, [Cat.] = 0.4 g/L, pH 2.1, vis	60	97	(Wang et al., 2015b)
NH ₂ -MIL-88B(Fe)	[Cr(VI)] = 8 mg/L, [Cat.] = 0.5 g/L, pH 2, T = 303 K, vis	45	100	(Shi et al., 2015)
NNU-36	[Cr(VI)] = 10 mg/L, [Cat.] = 0.375 g/L, pH 2.17, vis	60	95	(Zhao et al., 2017)
UiO-66(NH ₂)	[Cr(VI)] = 10 mg/L, [Cat.] = 0.5 g/L, pH 2, T = 303 K, vis	80	97	(Shen et al., 2013a, 2015)
Au@MIL-100(Fe)	[Cr(VI)] = 20 mg/L, [Cat.] = 1 g/L, pH 4, vis	20	100	(Liang et al., 2015b)
g-C ₃ N ₄ /MIL-53(Fe)	[Cr(VI)] = 10 mg/L, [Cat.] = 0.4 g/L, pH 2-3, vis	180	100	(Huang et al., 2017)
HPMo@MIL-100(Fe)	[Cr(VI)] = 20 mg/L, [Cat.] = 0.5 g/L, pH 4, vis	8	100	(Liang et al., 2015a)
MIL-53(Fe)-RGO	[Cr(VI)] = 20 mg/L, [Cat.] = 1 g/L, pH 4, vis	80	100	(Liang et al., 2015d)
Pd@MIL-100(Fe)	[Cr(VI)] = 20 mg/L, [Cat.] = 1 g/L, pH 4, vis	16	100	(Liang et al., 2015b)
Pd@UiO-66(NH ₂)	[Cr(VI)] = 10 mg/L, [Cat.] = 0.5 g/L, pH 2, T = 303 K, vis	90	99	(Shen et al., 2013b)
Pd-Cu/MIL-101	[Cr(VI)] = 20 mM, [Cat.] = 20 g/L, 0.3 mL HCOOH in 5 mL	60	100	(Trivedi et al., 2016)
Pd@MIL-101	[Cr(VI)] = 20 mM, [Cat.] = 3 g/L, 0.3 mL HCOOH in 5 mL, T = 323 K	210	100	(Yadav and Xu, 2013)
Pt@MIL-100(Fe)	[Cr(VI)] = 20 mg/L, [Cat.] = 1 g/L, pH 4, vis	8	100	(Liang et al., 2015b)
Pt@MIL-101	[Cr(VI)] = 20 mM, [Cat.] = 5.5 g/L, 0.3 mL HCOOH in 5 mL, T = 323 K	40	100	(Yadav and Xu, 2013)
RGO-UiO-66(NH ₂)	[Cr(VI)] = 10 mg/L, [Cat.] = 0.5 g/L, pH 2, T = 303 K, vis	100	100	(Shen et al., 2014)

Table 5. Summary of adsorptive capability of MOFs and MOF-based composites for radionuclides in water.

Metal species	Adsorbents (Ads.)	Reaction conditions	q_{\max} (mg/g)	Ref.
U(VI)	CMPO-MIL-101(Cr)	[U(VI)] = 30 mg/L, [Ads.] = 1 g/L, pH 4, T = 298 K	27.99	(De Decker et al., 2017)
	Co-SLUG-35	[U(VI)] = 20-500 mg/L, [Ads.] = 1 g/L, pH 9, T = 298 K	118	(Li et al., 2017)
	MIL-101	[U(VI)] = 5-200 mg/L, [Ads.] = 0.4 g/L, pH 5, T = 298 K	20	(Bai et al., 2015)
	MIL-101-NH ₂	[U(VI)] = 5-200 mg/L, [Ads.] = 0.4 g/L, pH 5, T = 298 K	90	(Bai et al., 2015)
	MIL-101-ED	[U(VI)] = 5-200 mg/L, [Ads.] = 0.4 g/L, pH 5, T = 298 K	200	(Bai et al., 2015)
	MIL-101-DETA	[U(VI)] = 5-200 mg/L, [Ads.] = 0.4 g/L, pH 5, T = 298 K	350	(Bai et al., 2015)
	MOF-3	[U(VI)] = 0-200 mg/L, [Ads.] = 1 g/L, pH 7, T = 318 K	314	(Li et al., 2016)
	MOF-76	[U(VI)] = 140 mg/L, [Ads.] = 0.4 g/L, pH 3	298	(Yang et al., 2013)
	1-NO ₂	[U(VI)] = 100 mg/L, [Ads.] = 0.5 g/L, pH 2, T = 298 K	165.3	(Song et al., 2016)
	Terbium(III)-based MOF	[U(VI)] = 5 mg/L, [Ads.] = 1 g/L, pH 4, RT	179.8	(Liu et al., 2017a)
	UiO-66	[U(VI)] = 5-120 mg/L, [Ads.] = 0.4 g/L, pH 5.5, RT	109.9	(Luo et al., 2016)
	UiO-66-NH ₂	[U(VI)] = 5-120 mg/L, [Ads.] = 0.4 g/L, pH 5.5, RT	114.9	(Luo et al., 2016)
	UiO-68-P(O)(OEt) ₂	[U(VI)] = 0-200 mg/L, [Ads.] = 1 g/L, RT	217 (pH 2.5); 152 (pH 5.0)	(Carboni et al., 2013)
	Zn(ADC)(4,4'-BPE) _{0.5} Zn(HBTC)(L)·(H ₂ O) ₂	[U(VI)] = 200 mg/L, [Ads.] = 0.5 g/L, pH 6 [U(VI)] = 100 mg/L, $M_{\text{adsorbent}} = 10$ mg, pH 2, T = 298 K	312.32 115	(Liu et al., 2016) (Wang et al., 2015)
	Se(IV)	NU-1000	[Se(IV)] = 18-55 mg/L, [Ads.] = 0.5 g/L, pH 6, T = 313 K	95
Se(VI)	NU-1000	[Se(VI)] = 18-55 mg/L, [Ads.] = 0.5 g/L, pH 6, T = 313 K	85	(Howarth et al., 2015)
Se(VI)	UiO-66-HCl	[Se(VI)] = 150 mg/L, [Ads.] = 1 g/L, pH 6.8	86.8	(Li et al., 2017)
Cs(I)	MIL-101-SO ₃ H	[Cs(I)] = 0.2 mM, [Ads.] = 1 g/L, pH 3, 6, 10	0.835	(Aguila et al., 2016)
	[(CH ₃) ₂ NH ₂][UO ₂ (L ₂)] ·0.5DMF·15H ₂ O	[Cs(I)] = 1-500 mg/L, [Ads.] = 1 or 5 g/L	145	(Wang et al., 2015)
Re(VII)	SBN	[Re(VII)] = 28 mg/L, [Ads.] = 0.5 g/L, pH 7	714	(Zhu et al., 2017b)
	SCU-100	[Re(VII)] = 28 mg/L, [Ads.] = 1 g/L	541	(Sheng et al., 2017)
	SLUG-21	[Re(VII)] = 200 mg/L, [Ads.] = 0.5 g/L, RT	602	(Fei et al., 2011)
	UiO-66-NH ₂	[Re(VII)] = 0.6 mM, [Ads.] = 1.2 mM, RT	159	(Banerjee et al., 2016)
Sr(II)	MIL-101-SO ₃ H	[Sr(II)] = 0.2 mM, [Ads.] = 1 g/L, pH 3, 6, 10	7.548	(Aguila et al., 2016)
Th(IV)	UiO-66-(COOH) ₂	[Th(IV)] = 5-200 mg/L, [Ads.] = 0.4 g/L, pH 3	350	(Zhang et al., 2017)

Note: CMPO, N,N-Diisobutyl-2-(octylphenylphosphoryl)acetamide; DETA, diethylenetriamine; L = N⁴,N^{4'}-di(pyridine-4-yl)biphenyl-4,4'-dicarboxamide).

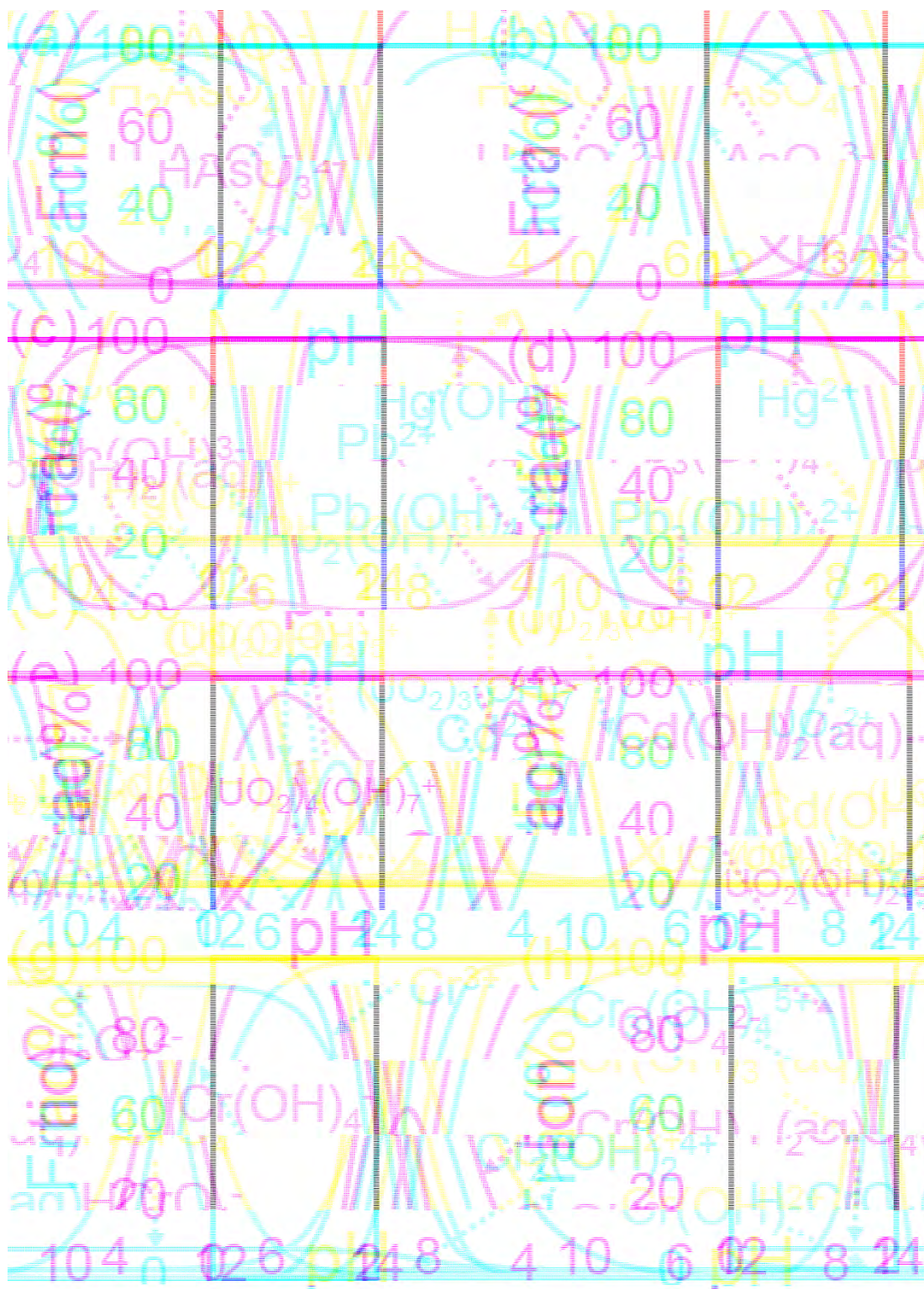


Fig. 1. The speciation distribution of the representative metal ions (a, As(III); b, As(V); c, Pb(II); d, Hg(II); e, Cd(II); f, U(VI); g, Cr(III); and h, Cr(VI); total concentration of each metal species was used as 0.01 mM) as a function of pH in water, which was plotted according to Visual MINTEQ 3.1.

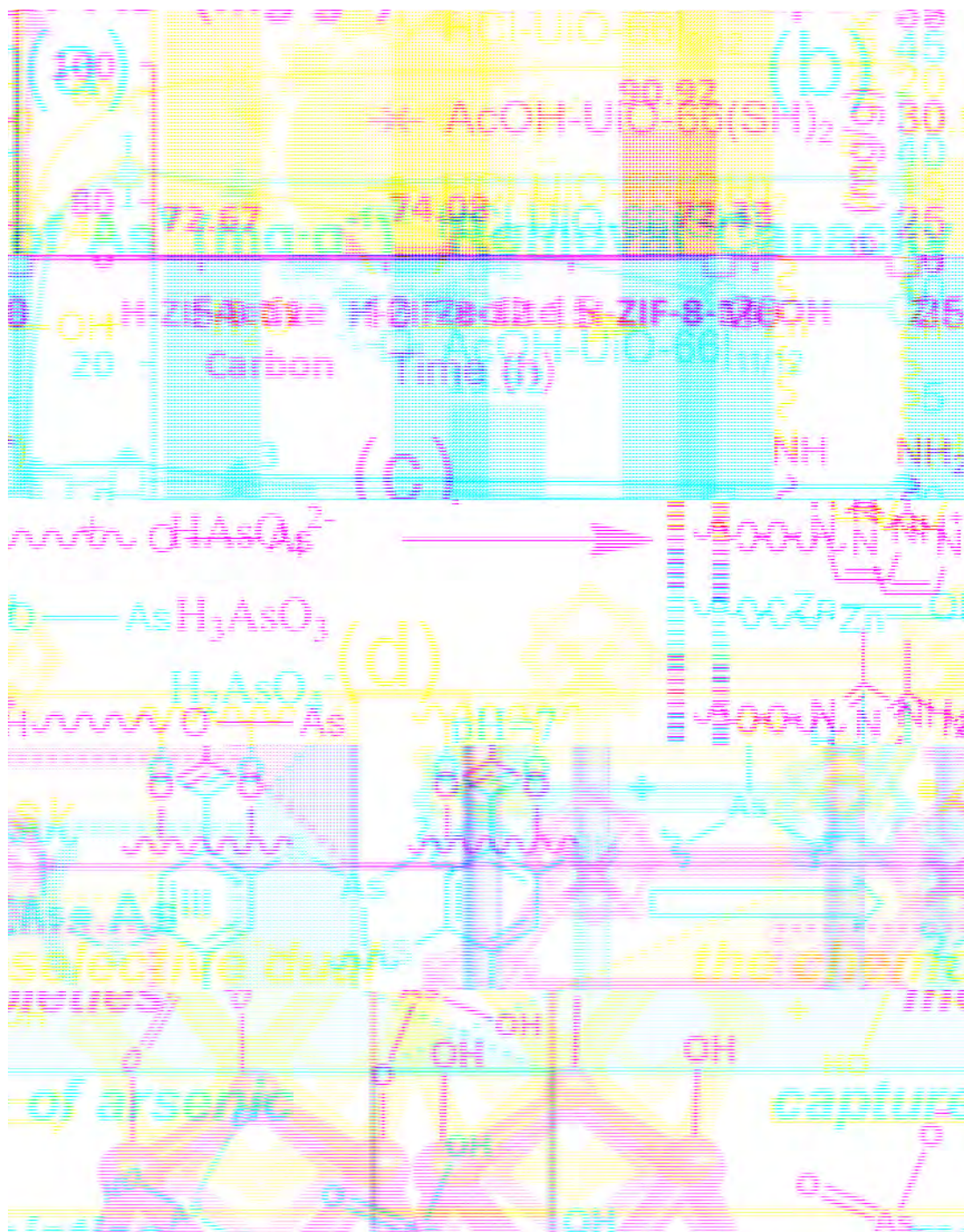


Fig. 2. (a) Comparison of the adsorptive removal of As(V) by commercial active carbon, zeolite, the synthesized ZIF-8, and hierarchically ZIF-8 with different molar ratios (1:1, 1:2 and 1:4) of [CTAB]:[His] in water, (b) aqueous uptake of As(III) by thiolated UiO-66 adsorbents and non-functionalized analogues, (c) schematic representation of the possible adsorptive process of As(III) and As(V) by ZIF-8 nanoparticles, (d) schematic diagram that shows how As(III) and As(V) can be individually captured by the organic linkers and nodes of UiO-66. (Adapted from (Audu et al., 2016; Jian et al., 2015; Wu et al., 2014) with permission from Elsevier Inc. and Royal Society of Chemistry).

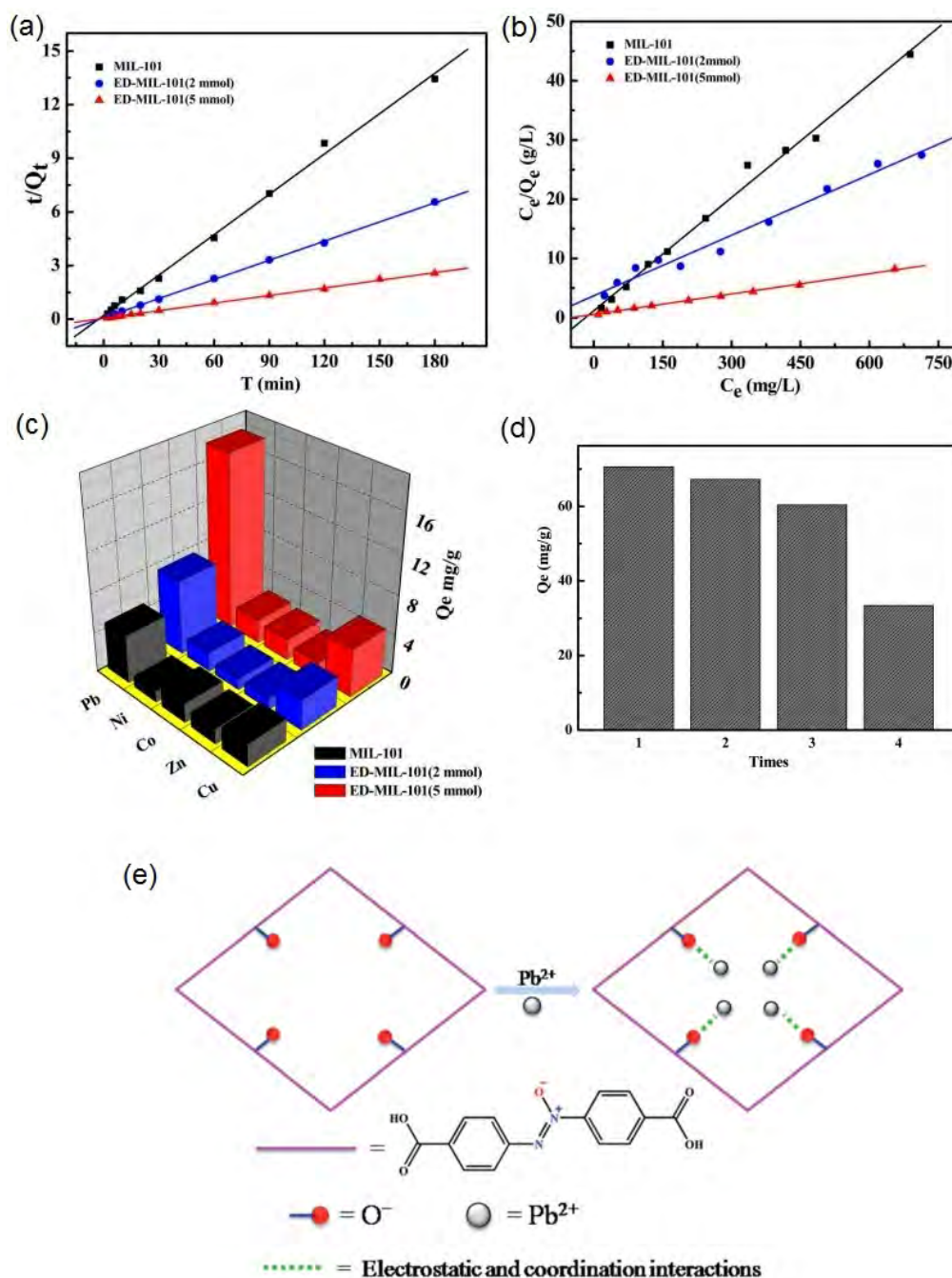


Fig. 3. (a) The pseudo-second-order kinetics, (b) Langmuir isotherms, and (c) selectivity for the adsorptive removal of Pb(II) by MIL-101(Cr), ED-MIL-101(Cr) (2 mmol) and ED-MIL-101(Cr) (5 mmol) as well as (d) reusability of ED-MIL-101(Cr) (5 mmol) during four successive runs of Pb(II) adsorption; (e) schematic diagram of the adsorptive mechanisms of Pb(II) by Zn(II)-based MOFs functionalized by O^- groups in water. (Adapted from (Luo et al., 2015; Yu et al., 2017) with permission from Elsevier Inc. and Royal Society of Chemistry).

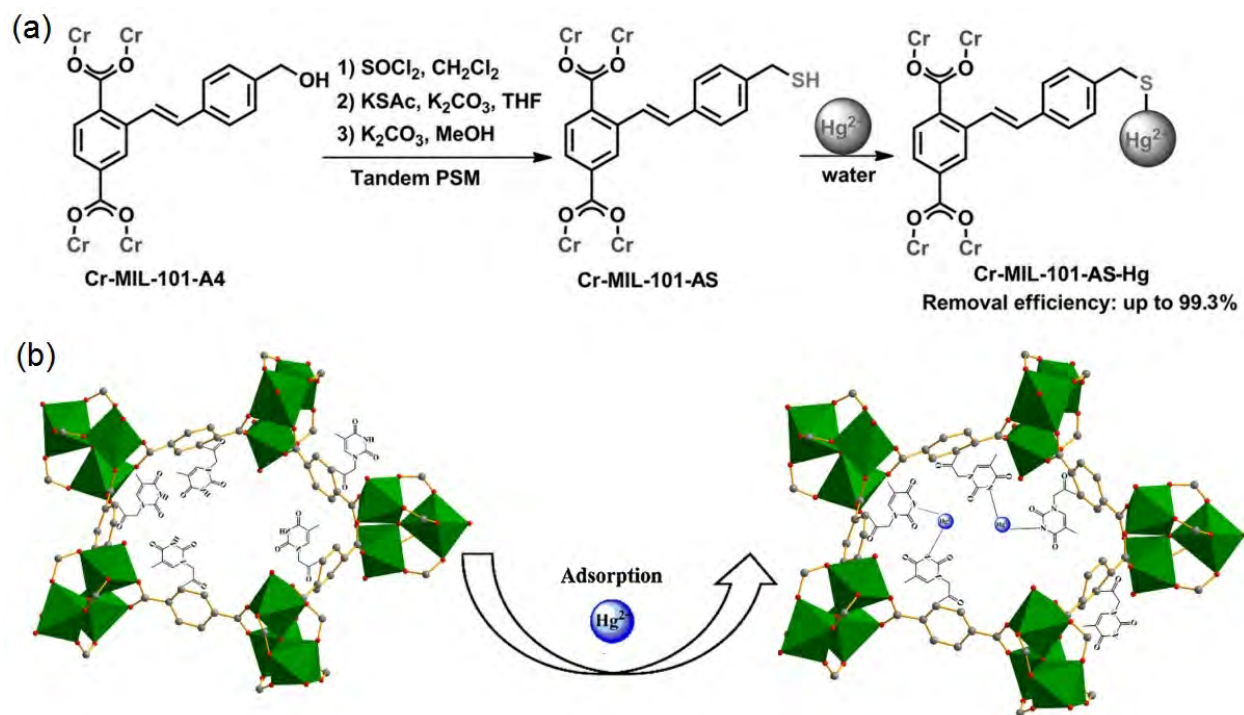


Fig. 4. (a) The post-synthetic modification of MIL-101(Cr) and its adsorption mechanism for Hg(II) in water; (b) aqueous adsorption mechanism of Hg(II) by MIL-101-Thymine. (Adapted from (Liu et al., 2014; Luo et al., 2016) with permission from Elsevier Inc. and Wiley).

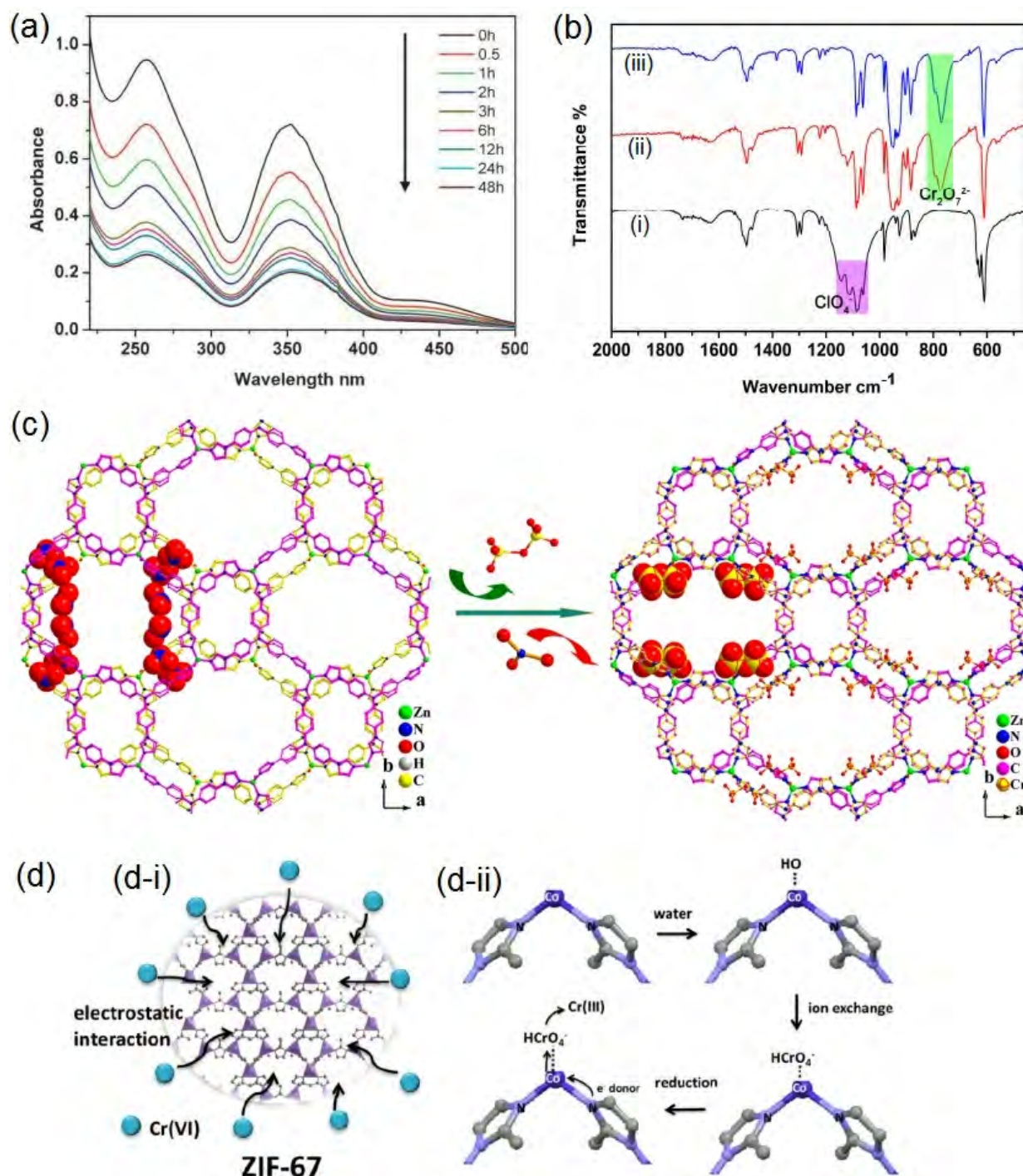


Fig. 5. (a) Change of UV/Vis spectra of Cr(VI) during exchange with equimolar ABT•2ClO₄ in water, (b) IR spectra of (i) as-prepared ABT•2ClO₄, (ii) ABT•2ClO₄ after immersing into equimolar Cr(VI) solution, and (iii) ABT•Cr₂O₇, (c) proposed structure changes of FIR-53 before and after ion exchange with Cr(VI) in water, (d) the possible adsorption mechanisms (d-i, electrostatic interaction, d-ii, ion exchange) of aqueous removal of Cr(VI) by ZIF-67. (Adapted from (Fu et al., 2015; Li et al., 2013, 2015) with permission from Wiley, American Chemistry Society and Elsevier Inc.).

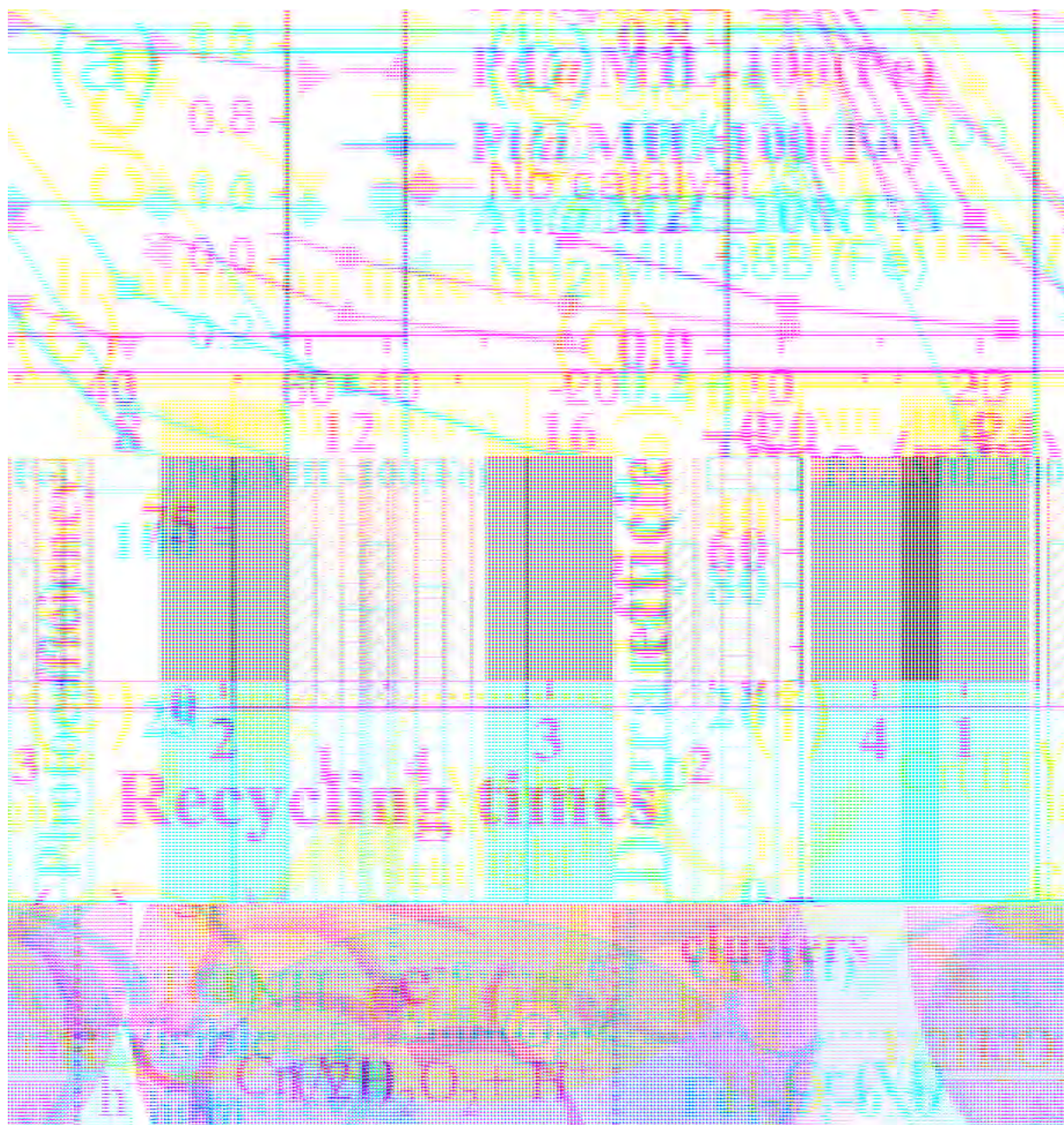


Fig. 6. Photocatalytic reduction of Cr(VI) by (a) MIL-88B(Fe), NH₂-UiO-66-Zr, NH₂-MIL-125-Ti, and NH₂-MIL-88B(Fe), (b) MIL-100(Fe) and M-MIL-100(Fe) (M = Au, Pd, and Pt) in water, and the reusability of (c) MIL-100(Fe) and M-MIL-100(Fe) (M = Au, Pd, and Pt) and (d) g-C₃N₄/MIL-53(Fe) for photocatalytic reduction of aqueous Cr(VI), (e) proposed mechanisms for dual excitation pathways of photocatalytic reduction of Cr(VI) using NH₂-MIL-88B(Fe), (f) schematic representation of the visible light-driven photocatalytic reduction of Cr(VI) by g-C₃N₄/MIL-53(Fe). (Adapted from (Huang et al., 2017; Liang et al., 2015b; Shi et al., 2015) with permission from Elsevier Inc., Wiley and Springer).



Fig. 7. Reductive conversion of Cr(VI) using excess of formic acid catalyzed by (a) 2 wt% M@MIL-101 (M = Pt, Pd, Au and Rh) at 323 K and (b) 2 wt% Pd-Cu@MIL-101 at room temperature, (c) schematic illustration of catalytic HCOOH reduction of Cr(VI) to Cr(III) by 2 wt% Pd-Cu@MIL-101, (d) the recycling performances with 2 wt% Pd_{0.5}-Cu_{0.5}@MIL-101 for catalytic Cr(VI) reduction into Cr(III). (Adapted from (Trivedi et al., 2016; Yadav and Xu, 2013) with permission from Royal Society of Chemistry.).

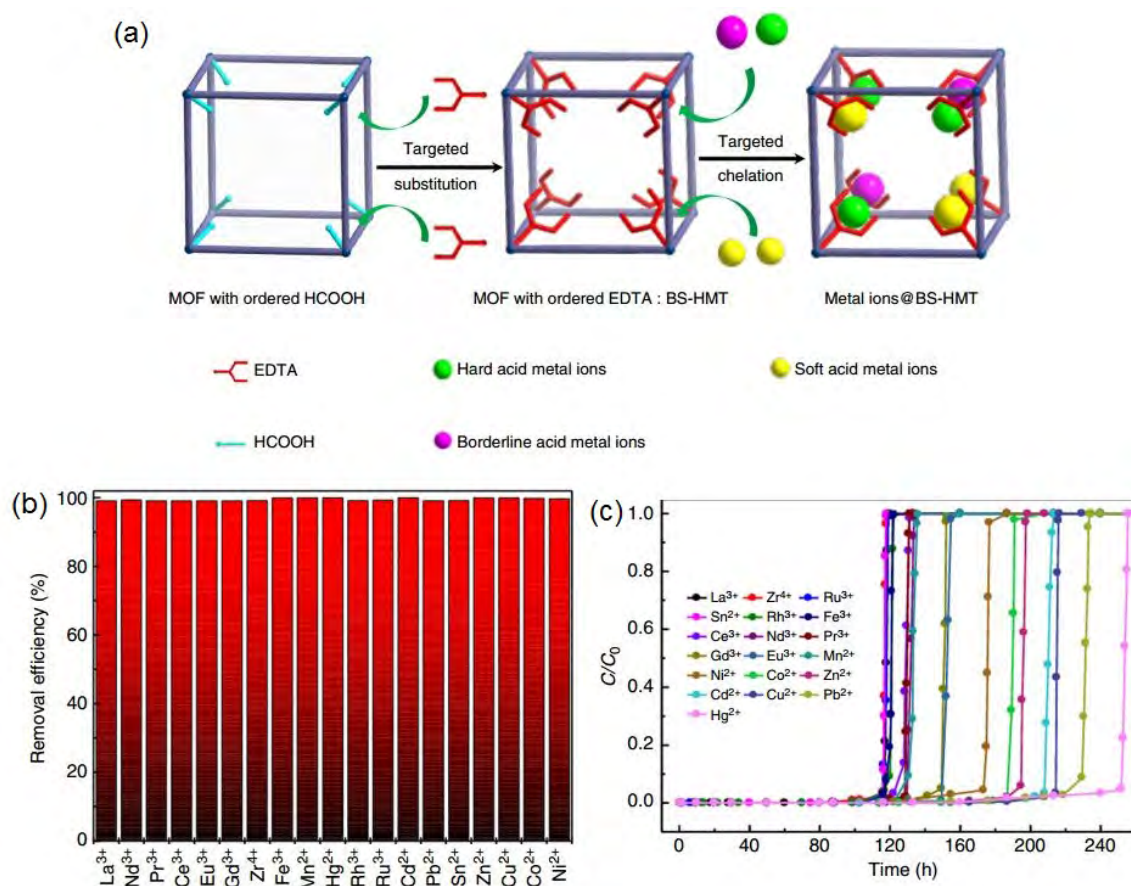


Fig. 8. (a) Schematic presentation of conceptual designation of broad-spectrum heavy metal ion trap (BS-HMT) by using EDTA-substituted MOF-808, (b) the capture efficiency of MOF-808-EDTA in multi-component aqueous system, (c) the adsorption curves of multiple heavy metals by MOF-808-EDTA in the fixed bed. (Adapted from (Peng et al., 2018) with permission from Nature Publishing Group.)

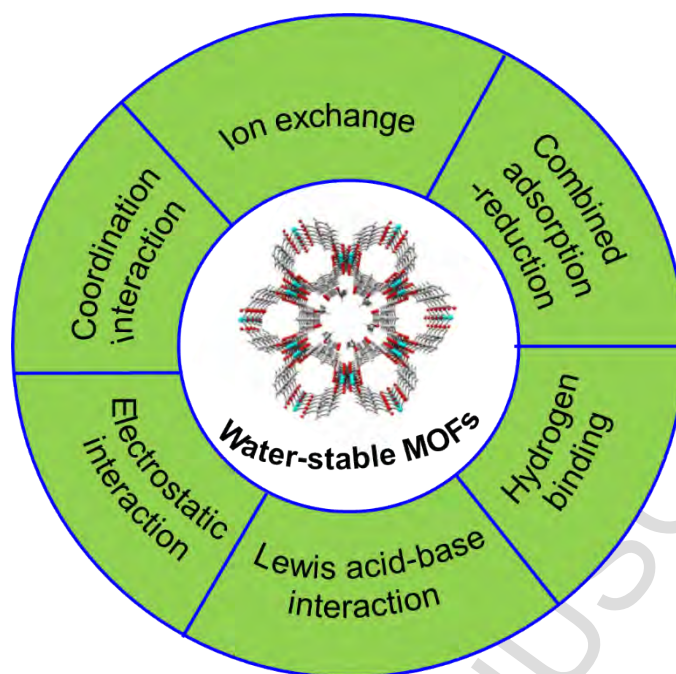


Fig. 9. The adsorption mechanisms of water-stable MOFs and MOF-based composites for heavy metals and radionuclides in water.

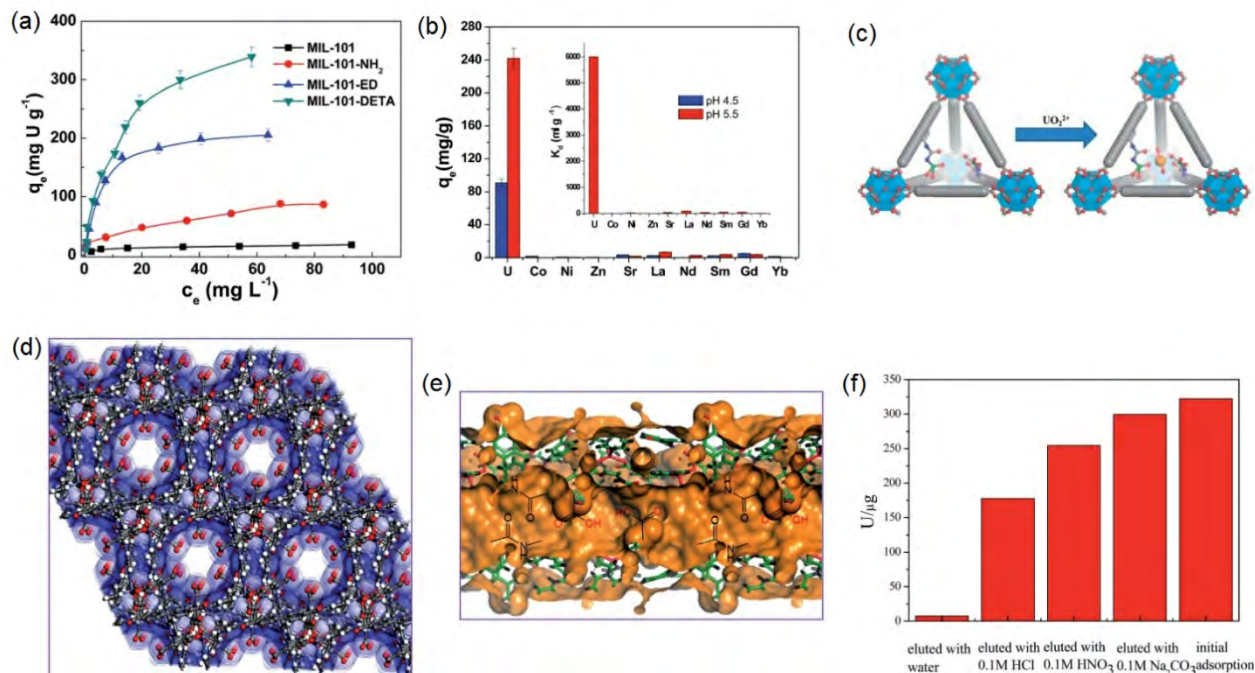


Fig. 10. (a) Effects of MIL-101(Cr) and its different functionalized analogues on aqueous removal of U(VI); (b) competitive adsorption and distribution coefficient (K_d) of multiple heavy metal ions by MIL-101-DETA; (c) schematic representation of the coordination of U(VI) with the phosphoryl oxygen of functionalized UiO-68 network; (d) the 3D framework of the MOF, Zn(HBTC)(L)·(H₂O)₂; (e) the 1D channel along the c axis and the inclusion of reactive ligands (acylamide and carboxyl units); (f) the elution efficiency of different solutions for the regeneration of Zn(HBTC)(L)·(H₂O)₂. (Adapted from (Bai et al., 2015; Carboni et al., 2013; Wang et al., 2015) with permission from Royal Society of Chemistry and Elsevier Inc.).



Fig. 11. (a) The number of Se(IV) and Se(VI) molecules adsorbed per node in different Zr-based MOFs, with the maximum possible adsorption and the actual adsorption individually presented in the light colored and dark colored bars; (b) the possible binding sites and modes of Se(IV) or Se(VI) to the node of NU-1000. (Adapted from (Howarth et al., 2015) with permission from American Chemistry of Society).

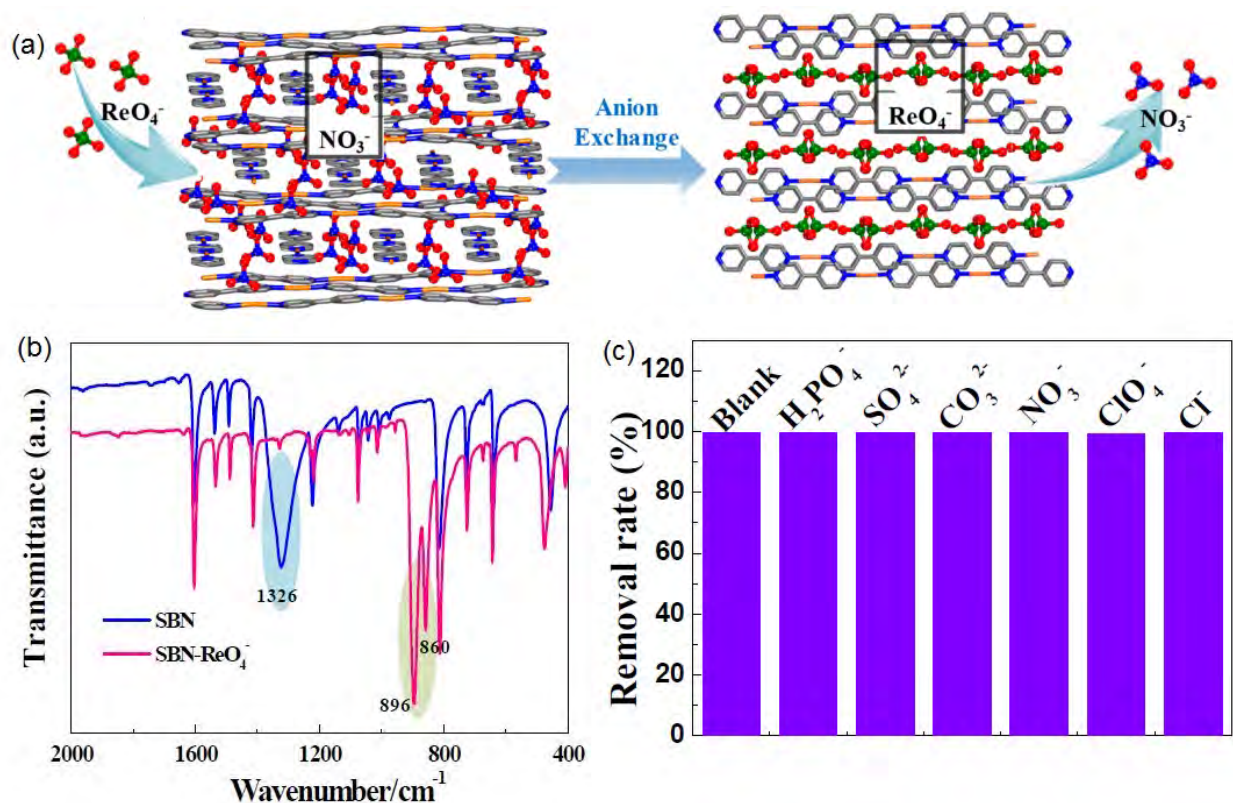


Fig. 12. (a) The SC-SC anion exchange mechanism of Re(VII) by SBN materials, (b) FT-IR spectra of SBN before and after Re(VII) capture, (c) the effect of different coexisting anions on aqueous removal of Re(VII) by SBN. (Adapted from (Zhu et al., 2017b) with permission from American Chemistry of Society).

Highlights

- Water-stable MOFs and MOF-based composites recover heavy metals and radionuclides
- Hazardous metal species can be efficiently adsorbed by MOFs.
- MOFs catalyze effectively photochemical conversion of chromium(VI)
- Green MOFs show high potential in sustainable water purification.